Metabolome Mining of Curcuma longa L. Using HPLC-MS/MS and Molecular Networking

Rabin Budhathoki , Arjun Prasad Timilsina , Bishnu P. Regmi , Khaga Raj Sharma , Niraj Aryal * , Niranjan Parajuli *

Posted Date: 27 June 2023

doi: 10.20944/preprints202306.1846.v1

Keywords: Untargeted metabolomics; HPLC-ESI-MS/MS; Curcuma longa; GNPS; Diarylheptanoids

Article

Metabolome Mining of *Curcuma longa* L. Using HPLC-MS/MS and Molecular Networking

Rabin Budhathoki[1], Arjun Prasad Timilsina[1], Bishnu P. Regmi[2], Khaga Raj Sharma[1], Niraj Aryal[3,*] and Niranjan Parajuli[1,*]

[1] Biological Chemistry Lab, Central Department of Chemistry, Tribhuvan University, Kirtipur, Kathmandu, 44618, Nepal; rabin.bc.992@gmail.com (R.B.); arzun1777@gmail.com (A.P.T.); khagaraj_sharma33@yahoo.com (K.R.S.); niranjan.parajuli@cdc.tu.edu.np (N.P.)
[2] Department of Chemistry, Florida Agricultural and Mechanical University, Tallahassee, FL 32307, USA; bishnu.regmi@famu.edu (B.P.R.)
[3] Department of Biology, University of Florida, Gainesville, FL 32611, USA; ; aryal.niraj3@gmail.com (N.A.)
* Correspondence: niraj.aryal@ufl.edu (N.A.); niranjan.parajuli@cdc.tu.edu.np (N.P.), Tel: +977-1-4332034

Abstract: Turmeric, *Curcuma longa* L., is a type of medicinal plant characterized by its perennial nature and rhizomatous growth. It is a member of the Zingiberaceae family and is distributed across the world's tropical and subtropical climates, especially in South Asia. Its rhizomes are highly valued for food supplements, spices, flavoring agents, and yellow dye in South Asia since ancient times. It exhibits a diverse array of therapeutic qualities that encompass its ability to combat diabetes, reduce inflammation, act as an antioxidant, exhibit anticancer properties, and promote anti-aging effects. In this study, organic extracts of *C. longa* rhizomes were subjected to HPLC separation followed by mass spectrometry analysis. The Global Natural Product Social Molecular Networking (GNPS) approach was utilized for the first time in this ethnobotanically important species to conduct an in-depth analysis of its metabolomes based on their fragments. A total of 30 metabolites including 16 diarylheptanoids, 1 diarylpentanoid, 3 bisabolocurcumin ethers, 4 sesquiterpenoids, 4 cinnamic acid derivatives, and 2 fatty acid derivatives were identified. Among 16 diarylheptanoids identified in this study, five of them are reported for the first time in this species.

Keywords: untargeted metabolomics; HPLC-ESI-MS/MS; *Curcuma longa*; GNPS; diarylheptanoids

1. Introduction

Curcuma longa L., a member of the family Zingiberaceace, is commonly referred to as turmeric and, is a perennial rhizomatous herbaceous plant, native and cultivated in the tropical region of Southeast Asian countries. It has been a part of South Asian culture, used for coloring, preservatives, and as a spice for more than 4,000 years. It is a popular ingredient in traditional medical practices, such as Siddha, Ayurveda, and Unani, commonly used as a natural remedy for various health conditions [1]. *C. longa* L. is rich in secondary metabolites and known to have antidiabetic, anticancer, antioxidant, anti-inflammatory, antibacterial, antifungal, antiviral, cardiovascular, and neuroprotective activities [2–4].

Diarylheptanoids and sesquiterpenoids are the major metabolites found in *C. longa* L. Diarylheptanoids are a distinct group of natural products comprising a heptane core structure with two phenyl rings at 1- and 7-positions. Due to the distinct characteristics of these compounds, various researchers have thoroughly investigated their therapeutic potential. The pharmacological activity of diarylheptanoids may be attributed to their high degree of flexibility in core

 doi:10.20944/preprints202306.1846.v1

chemical structure and the presence of few hydroxyl or ketone functionalities, thus making them tolerant to biological molecules [5].

Curcuminoids, a subclass of diarylheptanoids, include curcumin and its derivatives such as bisdemethoxycurcumin and demethoxycurcumin, which are natural phenols with therapeutic potential [6,7]. Curcumin, one of the most abundant curcuminoids with a long history of medicinal importance, is present in *Curcuma* species. It is found in high concentration in the rhizomes, making up about 3–6% of the dry weight [8].

The metabolic composition of plants may change in response to various physiological and environmental factors, and may also be influenced by their genetic makeup [9]. To analyze and compare all biological metabolites with molecular weights up to 1500 Da, metabolomics is an appealing tool. Metabolomics, which is a rapidly growing research field, comprises methods and techniques to analyze metabolites in biosynthetic pathways, thereby providing insights into the biochemical conditions of biological systems.

Targeted and untargeted approaches are the two strategies used in metabolomics. In targeted metabolomics, preselected specific metabolites are identified, whereas untargeted metabolomics involves the detection and identification of all metabolites, including unknown chemicals [10]. In the field of metabolomics, a combination of chromatography with mass spectrometry is regarded as the fundamental and essential analytical technique and it is frequently utilized due to its ability to analyze complex biological samples, as well as its large dynamic range and reproducibility [11,12]. Moreover, advancements in metabolomics have ramped up its development into a crucial tool in the medical field, particularly in the investigation of biomarkers associated with diseases, and toxic chemicals, and for the exploration of molecular mechanisms, or to deliver thorough insight into human biochemistry [13].

The complex MS/MS data acquired in metabolomics experiments can be visualized and analyzed employing a computer-based approach, molecular networking, that establishes a network-shaped map based on similarity in fragmentation patterns of two or more molecules. Global Natural Products Social Molecular Networking (GNPS) is a crucial bioinformatics online tool that is currently being utilized to perform molecular networking, and it can detect possible resemblance among all MS^2 datasets which further aids in the annotation of unknown but closely related metabolites [14].

Curcuma longa has been extensively investigated in the past for its metabolites [15–17]. Sesquiterpenoids and terpecurcumins extracted from *C. longa* L. have been studied for their anti-inflammatory, anti-atherosclerotic, and cytotoxic properties [18–20]. Recently, the antioxidant potential of diarylheptanoids has been explored [21,22]. Additionally, recent studies have analyzed metabolite differences between five *Curcuma* species using UPLC-MS/MS and reported that the quantity of curcuminoids in *C. longa* L. is higher than that in *Curcuma* species [23].

This research aimed to explore the secondary metabolites present in the rhizome of *Curcuma longa* L. through the application of high-performance liquid chromatography coupled with high-resolution tandem mass spectrometry (HPLC-MS/MS) and molecular networking techniques.

 doi:10.20944/preprints202306.1846.v1

2. Materials and Methods

2.1 Plant Collection and Extract Preparation

The fresh rhizomes of the *Curcuma longa* L. plant were collected from Bardiya district (GPS coordinates: 28.240525, 81.522853) of Lumbini province, Nepal, and were milled into fine powder. The pulverized powder was macerated with methanol. The powdered sample was subjected to a 24-hour soaking process in methanol, followed by filtration. The aforementioned procedure was repeated thrice; and, by setting the temperature of the rotatory evaporator at 40 °C the diluted extract was concentrated each time until a solid mass was obtained. Fractionation of crude extract was carried out by dissolving it into distilled water and subsequently extracted using ethyl acetate and hexane.

2.2 GNPS-based Molecular Networking

GNPS platform (https://gnps.ucsd.edu/) leverages complex MS/MS data in metabolomics experiments for the visualization and further annotation of metabolites based on similarity in fragmentation patterns [24]. The raw data files (.d format) in positive ionization mode of ethyl acetate and hexane fractions were first converted to .mzXML format using open-source MSConvert software (Version: 3.0). The converted files were uploaded to Mass Spectrometry Interactive Virtual Environment (MassIVE) dataset (https://massive.ucsd.edu/)(Accession number: MSV000092243) using FTP client CoffeeCup. The precursor ion and fragment ion mass tolerance was set at 2.0 Da and 0.5 Da, respectively. Then, GNPS was performed to construct a network by setting the cosine score value greater than 0.7. The generated molecular networks were then exported to Cytoscape software (Version: 3.10.0) in '.graphml' format to visualize the networks.

2.3 Mass Spectrometry and Compound Annotation

The high-performance liquid chromatography-high resolution-mass spectrometry (HPLC-HR-MS/MS) based metabolic profiling of ethyl acetate and hexane fractions of *C. longa* rhizome was carried out on a Bruker Maxis Impact ESI mass spectrometer as described in a prior study carried out at Gross lab, the University of Tübingen, Germany by Aryal et al. [25]. Both modes of ionization were employed to measure HRMS data. The raw data was manually skimmed for quality and then analyzed in Bruker Compass Data Analysis (Version 4.4, Bruker Daltonics GmbH, Billerica, MA, USA). Subsequently, raw data files were converted into .mzXML format and further annotated using CSI: FingerID (a graphical user interface for SIRIUS) [26]. The calculated mass, absolute error, RDBE, and molecular formulae were generated by using Bruker Data Analysis software and were compared to the formula generated by SIRIUS. Furthermore, the annotated compounds were validated via the SIRIUS score, and literature survey along with natural products-based servers and databases; PubChem [27], LOTUS [28], and ChemSpider [29]. The higher the value of the SIRIUS score, the higher the confidence of molecular annotation.

3. Results

Preprints (www.preprints.org) | NOT PEER-REVIEWED | Posted: 27 June 2023 doi:10.20944/preprints202306.1846.v1

3.1. Metabolite Profiling Using HPLC-MS/MS

The LC-HR-ESI-MS/MS-based metabolite profiling of the rhizomes of *C. longa* L. displayed a significant abundance of therapeutically active compounds belonging to various classes including phenolic compounds, cinnamic acid derivatives, sesquiterpenoids, and fatty acids. The base peak chromatograms of ethyl acetate fraction for positive and negative modes of ionization are shown in Figure 1 and Figure 2, respectively.

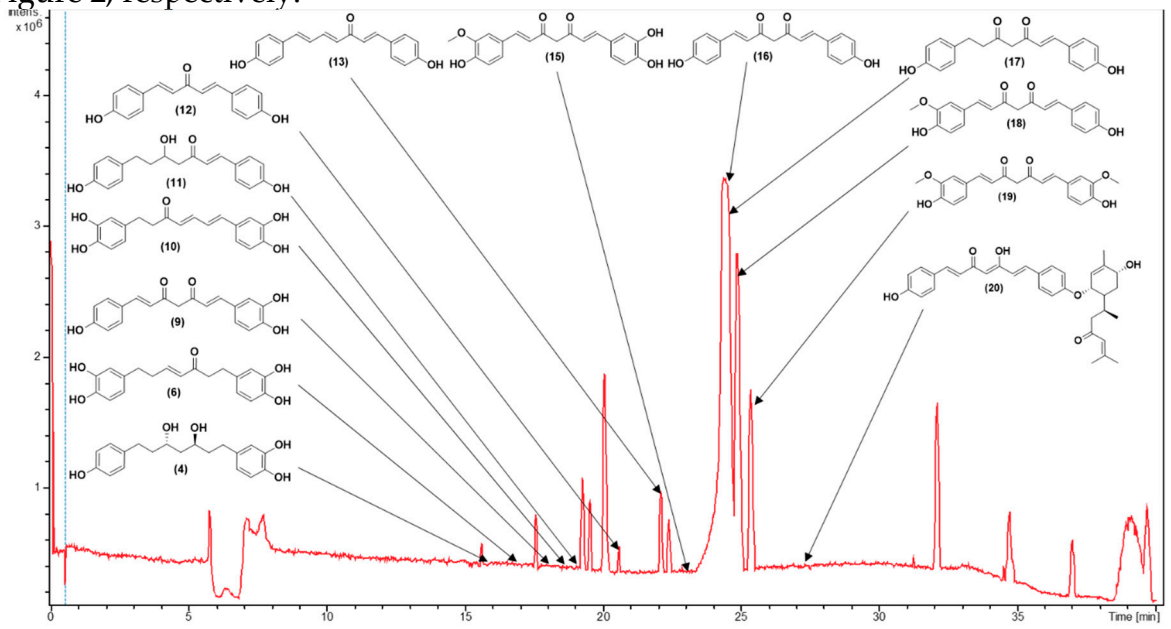

Figure 1. Base peak chromatogram for ethyl acetate fraction in (+)-ESI mode, portraying annotated diarylheptanoids from the *C. longa* rhizome.

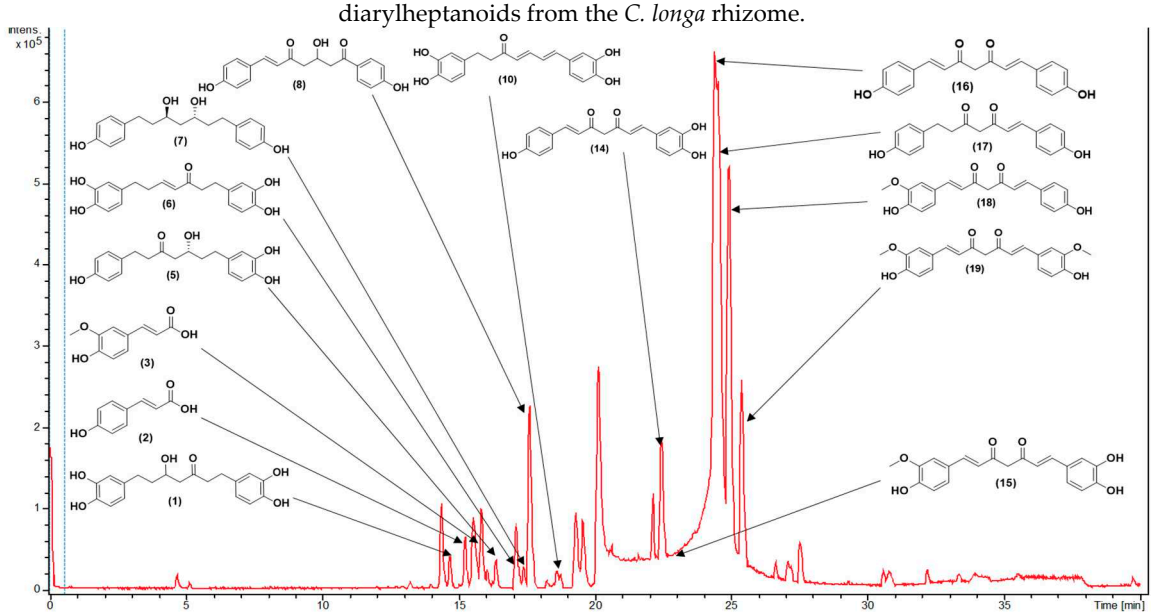

Figure 2. Base peak chromatogram for ethyl acetate fraction in (–)-ESI mode, portraying annotated met from the *C. longa* rhizome.

A total of 30 secondary metabolites annotated from HR-MS data of ethyl acetate and hexane fractions ionized in both positive and/or negative modes are listed in Table 1 and Table 2, respectively.

The MS^1 and MS^2 profiles of the observed metabolites are displayed in Supplementary Figures S1—S30. The structures of annotated metabolites are displayed in Figure 3.

Preprints (www.preprints.org) | NOT PEER-REVIEWED | Posted: 27 June 2023 doi:10.20944/preprints202306.1846.v1

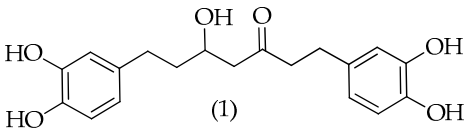

(1)
Exact Mass: 346.142
1,7-bis(3,4-dihydroxyphenyl)-5-hydroxyheptan-3-one

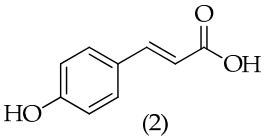

(2)
Exact Mass: 164.047
4-hydroxycinnamic acid

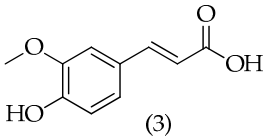

(3)
Exact Mass: 194.058
Ferulic acid

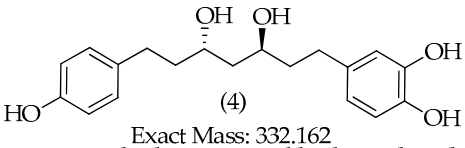

(4)
Exact Mass: 332.162
3,5-Dihydroxy-1-(3,4-dihydroxyphenyl)
-7-(4-hydroxyphenyl)heptane

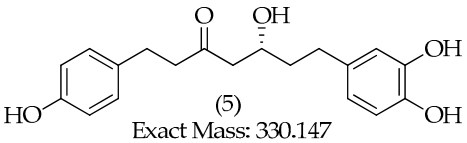

(5)
Exact Mass: 330.147
5-Hydroxy-1-(4-hydroxyphenyl)
-7-(3,4-dihydroxyphenyl)-3-heptanone

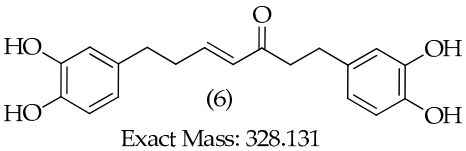

(6)
Exact Mass: 328.131
1,7-bis(3,4-dihydroxyphenyl)hept-4-en-3-one

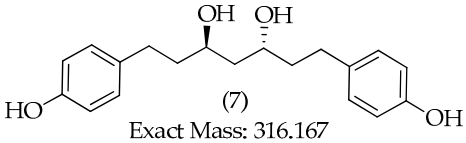

(7)
Exact Mass: 316.167
(3R,5R)-1,7-Bis(4-hydroxyphenyl)-3,5-heptanediol

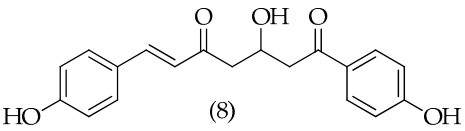

(8)
Exact Mass: 326.115
3-hydroxy-1,7-bis(4-hydroxyphenyl)-6-heptene-1,5-dione

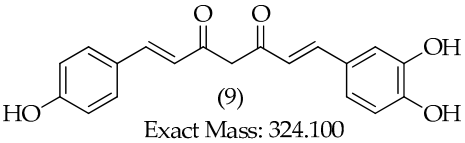

(9)
Exact Mass: 324.100
1-(4-hydroxyphenyl)-7-(3,4-dihydroxyphenyl)
-1,6-heptadiene-3,5-dione

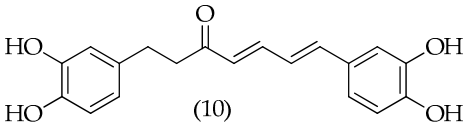

(10)
Exact Mass: 326.115
1,7-bis(3,4-dihydroxyphenyl)hepta-4,6-dien-3-one

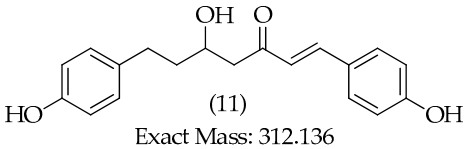

(11)
Exact Mass: 312.136
5-hydroxy-1,7-bis(4-hydroxyphenyl)hept-1-en-3-one

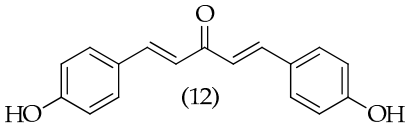

(12)
Exact Mass: 266.094
1,5-Bis(4-hydroxyphenyl)-1,4-pentadien-3-one

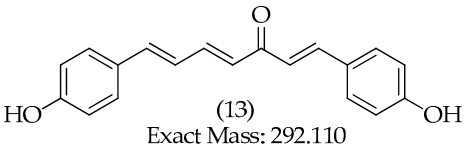

(13)
Exact Mass: 292.110
1,7-Bis(4-hydroxylphenyl)-1,4,6-heptatriene-3-one

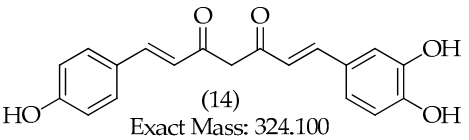

(14)
Exact Mass: 324.100
1-(3,4-dihydroxyphenyl)-7-(4-hydroxyphenyl)hepta
-1,6-diene-3,5-dione

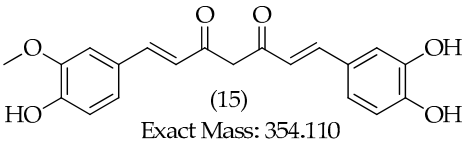

(15)
Exact Mass: 354.110
Monodemethylcurcumin

Preprints (www.preprints.org) | NOT PEER-REVIEWED | Posted: 27 June 2023 doi:10.20944/preprints202306.1846.v1

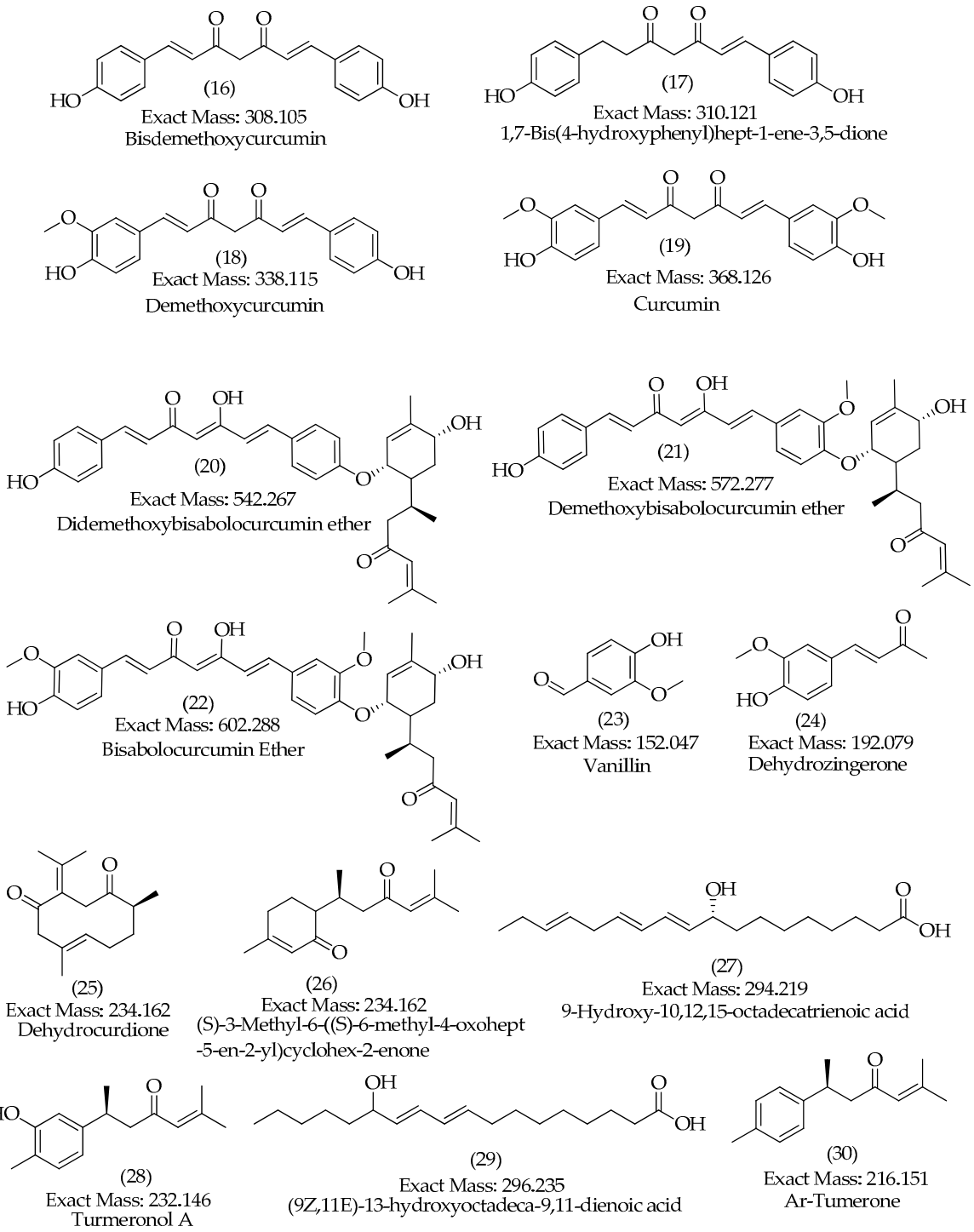

Figure 3. Chemical structures of annotated metabolites in the *C. longa* L. rhizomes using LC-HR-ESI-MS/MS.

Table 1. Secondary metabolites annotated in positive and/or negative mode in ethyl acetate fraction of *C. longa* L.

C. N.	RT(Min)	Detected Ion/adduct	Observed m/z	Calculated m/z	Error (ppm)	RDBE	MS² ion(m/z)	Mol. Formula	Predicted Metabolites	CSI:FingerID score (%)

 doi:10.20944/preprints202306.1846.v1

1	14.7	[M-H]⁻	345.1340	345.1344	0.9	9	345, 209, 191, 165, 161, 135 (bp)	$C_{19}H_{22}O_6$	1,7-bis(3,4-dihydroxyphenyl)-5-hydroxyheptan-3-one	81.08
2	15.3	[M+H]⁺	165.0551	165.0546	-2.8	6	147, 119 (bp), 91, 65	$C_9H_8O_3$	4-hydroxycinnamic acid	97.08
	15.3	[M-H]⁻	163.0401	163.0401	-0.1	6	119 (bp), 93	$C_9H_8O_3$	4-hydroxycinnamic acid	97.79
3	15.7	[M+H]⁺	195.0657	195.0652	-2.7	6	177, 163, 149, 145 (bp), 134, 117, 106, 89	$C_{10}H_{10}O_4$	Ferulic acid	98.90
	15.7	[M-H]⁻	193.0508	193.0506	-1.0	6	178, 134 (bp)	$C_{10}H_{10}O_4$	Ferulic acid	97.79
4	15.8	[M+H]⁺	333.1705	333.1697	-2.6	8	203, 187, 163, 149, 133, 123, 107 (bp)	$C_{19}H_{24}O_5$	3,5-Dihydroxy-1-(3,4-dihydroxyphenyl)-7-(4-hydroxyphenyl)heptane	97.35
	15.8	[M-H]⁻	331.1552	331.1551	-0.2	8	331 (bp)	$C_{19}H_{24}O_5$	3,5-Dihydroxy-1-(3,4-dihydroxyphenyl)-7-(4-hydroxyphenyl)heptane	93.65
5	16.4	[M-H]⁻	329.1394	329.1394	0.0	9	283, 161, 135 (bp)	$C_{19}H_{22}O_5$	5-Hydroxy-1-(4-hydroxyphenyl)-7-(3,4-dihydroxyphenyl)-3-heptanone	82.20
6	17.1	[M+H]⁺	329.1392	329.1384	-2.6	10	215, 179, 163 (bp), 145, 133, 107	$C_{19}H_{20}O_5$	1,7-bis(3,4-dihydroxyphenyl)hept-4-en-3-one	88.14
	17.1	[M-H]⁻	327.1239	327.1238	-0.4	10	177 (bp), 135	$C_{19}H_{20}O_5$	1,7-bis(3,4-dihydroxyphenyl)hept-4-en-3-one	71.43
7	17.4	[M-H]⁻	315.1602	315.1602	0.0	8	193, 163, 149 (bp), 147, 121, 112, 106, 93	$C_{19}H_{24}O_4$	(3R,5R)-1,7-bis(4-hydroxyphenyl)-3,5-heptanediol	95.42

 doi:10.20944/preprints202306.1846.v1

8	17.7	$[M-H]^-$	325.1082	325.1081	0.0	11	307, 239, 213, 187, 161, 145 (bp), 135, 119, 93, 68	$C_{19}H_{18}O_5$	3-hydroxy-1,7-bis(4-hydroxyphenyl)-6-heptene-1,5-dione	73.39
9	18.3	$[M+H]^+$	325.1080	325.1071	-3.0	12	279, 241, 223, 189, 163, 147 (bp), 131, 107	$C_{19}H_{16}O_5$	1-(4-hydroxyphenyl)-7-(3,4-dihydroxyphenyl)-1,6-heptadiene-3,5-dione	61.61
10	18.6	$[M+H]^+$	327.1233	327.1227	-1.9	11	257, 205, 189, 163, 149, 131, 123 (bp)	$C_{19}H_{18}O_5$	1,7-bis(3,4-dihydroxyphenyl)hepta-4,6-dien-3-one	80.73
	18.7	$[M-H]^-$	325.1081	325.1081	0.0	11	325,203 (bp),135, 119	$C_{19}H_{18}O_5$	1,7-bis(3,4-dihydroxyphenyl)hepta-4,6-dien-3-one	80.77
11	18.7	$[M+H]^+$	313.1441	313.1441	-2.2	10	235, 193, 163, 147 (bp), 133, 119, 107	$C_{19}H_{20}O_4$	5-hydroxy-1,7-bis(4-hydroxyphenyl)hept-1-en-3-one	63.93
	18.8	$[M-H]^-$	311.1288	311.1289	0.3	10	311, 190, 174, 161 (bp), 149, 119	$C_{19}H_{20}O_4$	5-hydroxy-1,7-bis(4-hydroxyphenyl)hept-1-en-3-one	65.42
12	20.6	$[M+H]^+$	267.1021	267.1016	-2.1	11	249, 231, 199, 173, 147 (bp), 119, 107, 91	$C_{17}H_{14}O_3$	1,5-bis(4-hydroxyphenyl)-1,4-pentadien-3-one	78.98
13	22.2	$[M+H]^+$	293.1178	293.1172	-2.1	12	225, 199, 181, 147, 131, 121, 107 (bp)	$C_{19}H_{16}O_3$	1,7-bis(4-hydroxyphenyl)-1,4,6-heptatrien-3-one	69.23
	22.2	$[M-H]^-$	291.1029	291.1027	-0.5	12	291, 249, 223, 211, 197, 185, 171(bp),	$C_{19}H_{16}O_3$	1,7-bis(4-hydroxyphenyl)-1,4,6-heptatrien-3-one	66.48

							145, 119, 93			
14	22.4	[M-H]⁻	323.0928	323.0925	-1.2	12	159, 143, 135 (bp), 119	$C_{19}H_{16}O_5$	1-(3,4-dihydroxyphenyl)-7-(4-hydroxyphenyl)hepta-1,6-diene-3,5-dione	59.09
15	22.8	[M+H]⁺	355.1185	355.1176	-2.5	12	353, 305, 271 (bp), 253, 239, 211, 177, 163, 145, 119, 68	$C_{20}H_{18}O_6$	Monodemethylcurcumin	75.54
	22.8	[M-H]⁻	353.1034	353.1031	-1.1	12	307, 217, 187, 173, 158, 145, 135 (bp), 119	$C_{20}H_{18}O_6$	Monodemethylcurcumin	75.56
16	23.9	[M+H]⁺	309.1127	309.1121	-1.7	12	225, 205, 189, 147 (bp), 131, 119, 107	$C_{19}H_{16}O_4$	Bisdemethoxycurcumin	93.42
	24.2	[M-H]⁻	307.0979	307.0976	-0.7	12	187, 143, 119 (bp)	$C_{19}H_{16}O_4$	Bisdemethoxycurcumin	96.13
17	24.2	[M+H]⁺	311.1280	311.1278	-0.8	11	225, 205, 189, 147 (bp), 131, 119, 107	$C_{19}H_{18}O_4$	1,7-bis(4-hydroxyphenyl)hept-1-ene-3,5-dione	75.56
	24.2	[M-H]⁻	309.1132	309.1132	0.2	11	189, 187, 161, 145, 143, 119 (bp)	$C_{19}H_{18}O_4$	1,7-bis(4-hydroxyphenyl)hept-1-ene-3,5-dione	80.43
18	24.8	[M+H]⁺	339.1229	339.1227	-0.6	12	289, 255, 195, 177 (bp), 147, 131, 119, 107	$C_{20}H_{18}O_5$	Demethoxycurcumin	99.50
	25.0	[M-H]⁻	337.1085	337.1081	-1.0	12	217, 202, 187, 173,	$C_{20}H_{18}O_5$	Demethoxycurcumin	98.07

Preprints (www.preprints.org) | NOT PEER-REVIEWED | Posted: 27 June 2023 doi:10.20944/preprints202306.1846.v1

							158, 149, 119 (bp)			
19	25.3	$[M+H]^+$	369.1337	369.1333	-1.2	12	285, 268, 225, 177 (bp), 161, 145, 137, 117	$C_{21}H_{20}O_6$	Curcumin	95.00
	25.3	$[M-H]^-$	367.1190	367.1187	-0.7	12	217, 202, 173, 158, 149 (bp), 134, 119	$C_{21}H_{20}O_6$	Curcumin	100
20	27.0	$[M+H]^+$	543.2747	543.2741	-1.2	16	349, 309, 229, 189, 147 (bp), 119	$C_{34}H_{38}O_6$	Didemethoxybisabolocurcumin ether	63.29
21	30.1	$[M+Na]^+$	595.2675	-	-	-	360, 257 (bp), 239	$C_{35}H_{40}O_7$	Demethoxybisabolocurcumin ether	-
22	30.7	$[M+Na]^+$	625.2786	-	-	-	301, 294, 257 (bp), 239	$C_{36}H_{42}O_8$	Bisabolocurcumin Ether	-

bp= base peak, C.N.= compound number

Table 2. Secondary metabolites annotated in positive and/or negative mode in hexane fraction of *C. longa* L. rhizomes.

C. N.	RT(Min)	Detected Ion/adduct	Observed m/z	Calculated m/z	Error (ppm)	RDBE	MS^2 ion(m/z)	Mol. Formula	Predicted Metabolites	CSI:FingerID score (%)
23	16.0	$[M+H]^+$	153.0547	153.0546	-0.7	5	125, 111, 93(bp),65	$C_8H_8O_3$	Vanillin	98.80
	16.0	$[M-H]^-$	151.0339	151.0401	1.1	5	136(bp), 108, 92	$C_8H_8O_3$	Vanillin	92.81
24	18.2	$[M-H]^-$	191.0712	191.0714	0.7	6	176(bp),	$C_{11}H_{12}O_3$	Dehydroxingerone	98.29

Preprints (www.preprints.org) | NOT PEER-REVIEWED | Posted: 27 June 2023 doi:10.20944/preprints202306.1846.v1

							148, 133			
25	24.5	$[M+H]^+$	235.1688	235.1693	1.8	5	161, 135, 121, 119(bp), 107, 105, 93, 83	$C_{15}H_{22}O_2$	Dehydrocurdione	65.84
26	26.4	$[M+H]^+$	235.1697	235.1693	-2.0	5	231, 213, 198, 175, 158, 147, 133(bp), 107, 97	$C_{15}H_{22}O_2$	(6s)-6-methyl-5-(3-oxobutyl)-2-(propan-2-ylidene)cyclohept-4-en-1-one	63.92
27	28.0	$[M-H]^-$	293.2125	293.2122	-1.0	4	293, 275(bp), 235, 231, 223, 183, 171, 121	$C_{18}H_{30}O_3$	9-Hydroxy-10,12,15-octadecatrienoic acid	98.76
28	28.5	$[M+H]^+$	233.1534	233.1536	0.7	6	145, 135, 131, 120, 119(bp), 117, 91, 83	$C_{15}H_{20}O_2$	Turmerone A	49.50

Preprints (www.preprints.org) | NOT PEER-REVIEWED | Posted: 27 June 2023 doi:10.20944/preprints202306.1846.v1

29	29.6	[M-H]⁻	295.2282	295.2279	-1.3	3	295, 277(bp), 195, 183, 171	$C_{18}H_{32}O_3$	Coriolic acid	95.76
30	31.2	[M+H]⁺	217.1588	217.1587	-0.3	6	120, 119(bp), 117, 109, 103, 91, 83, 67	$C_{15}H_{20}O$	Ar-Tumerone	93.66

bp= base peak, C.N.= compound number

2.2. Characterization of Compounds 1, 4, 5, 6 and 10

In our study, we observed diarylheptanoid compounds 1, 4, 5, 6, and 10 in turmeric for the first time. In (–)-ESI mode, compound 1 exhibited a molecular ion peak at the retention time of 14.7 minutes with *m/z* 345.1342 $[M-H]^-$. Its MS^2 profile (Figure 4a) revealed a base peak with *m/z* 135 $[M-H-C_{11}H_{12}O_4-H_2]^-$ corresponding to the $C_8H_7O_2^-$ ion formed by the elimination of $C_{11}H_{12}O_4$ unit and H_2 simultaneously.

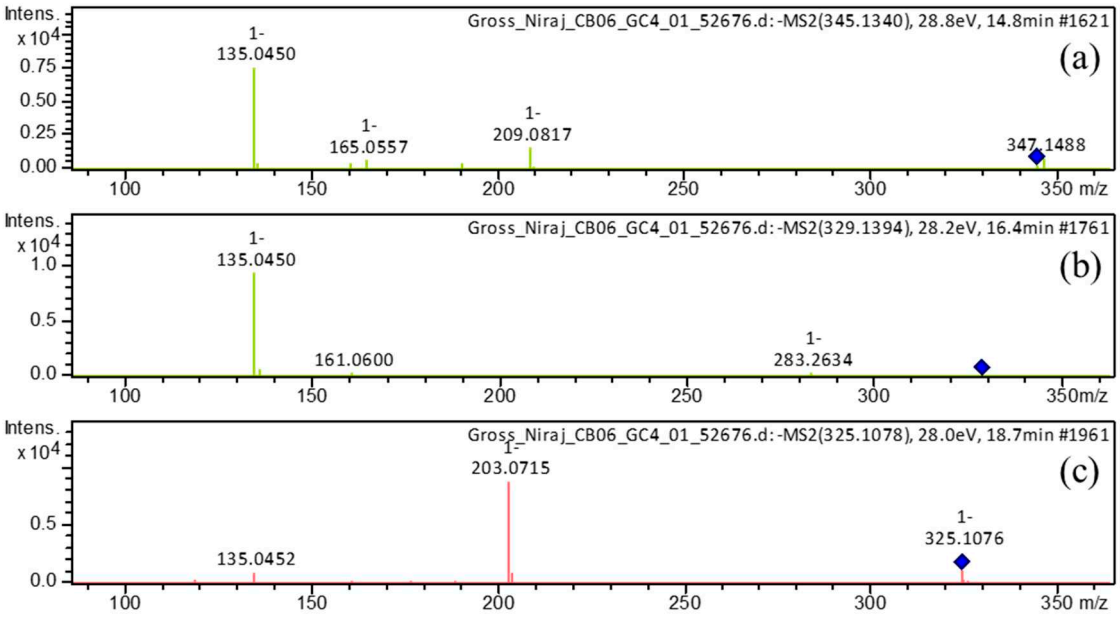

Figure 4. MS^2 profiles in (–)-ESI mode for: (a) Compound 1, (b) Compound 5, and (c) Compound 10.

Furthermore, fragment ions (Figure 5) were detected at *m/z* 165 because of $[M-H-C_{10}H_{12}O_3]^-$ and *m/z* 209 owing to $[M-H-C_8H_8O_2]^-$. Thus, compound 1 was identified as 1,7-bis(3,4-dihydroxyphenyl)-5-hydroxyheptan-3-one.

Preprints (www.preprints.org) | NOT PEER-REVIEWED | Posted: 27 June 2023 doi:10.20944/preprints202306.1846.v1

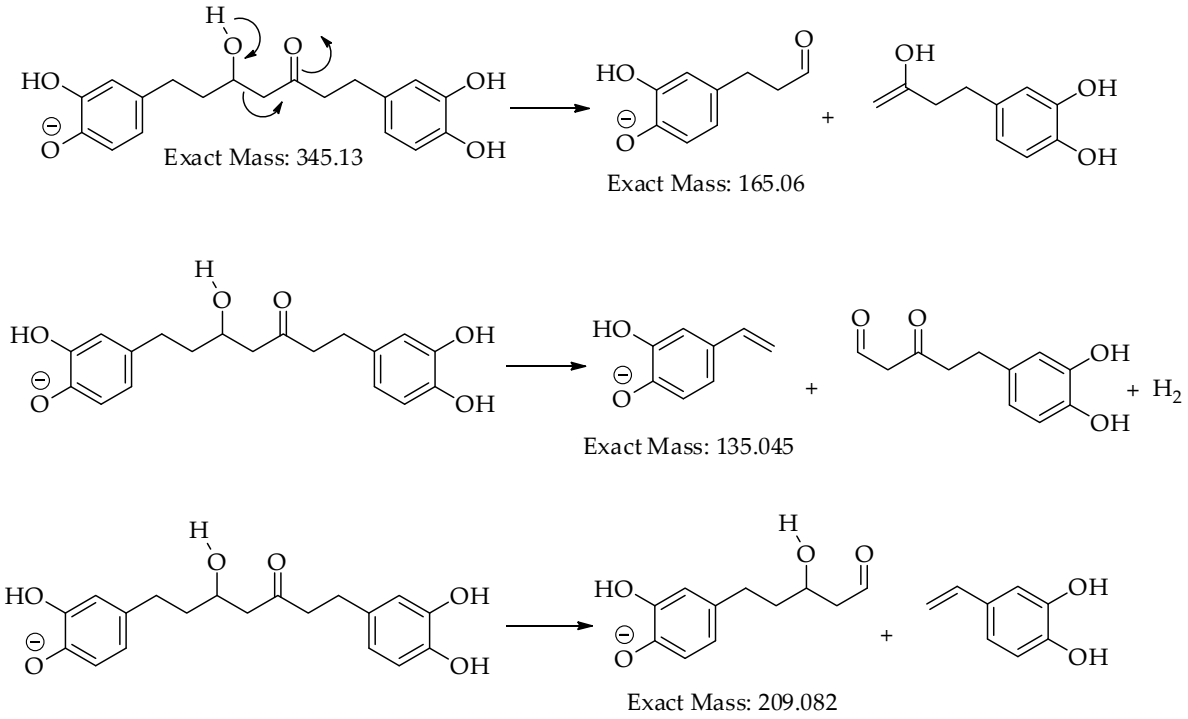

Figure 5. Observed fragmentation pattern of compound 1 in (–)-ESI mode.

Compound 4 displayed molecular ions with *m/z* 333.1705 $[M+H]^+$ and *m/z* 331.1552 $[M-H]^-$ in (+)-ESI and (–)-ESI modes respectively at retention time 15.8 min. Its MS^2 profile in positive mode (Figure 6a) showed characteristic fragments peaks with *m/z* 107 as a base peak due to removal of a water molecule followed by elimination of $C_{12}H_{16}O_3$ moiety i.e $[M+H-H_2O-C_{12}H_{16}O_3]^+$, *m/z* 123 attributed to $[M+H-H_2O-C_{12}H_{16}O_2]^+$ and *m/z* 149 due to $[M+H-H_2O-H_2-C_{10}H_{12}O_2]^+$. Thus, we identified compound 4 as 3,5-dihydroxy-1-(3,4-dihydroxyphenyl)-7-(4-hydroxyphenyl)heptane based on fragment ions (Figure 7).

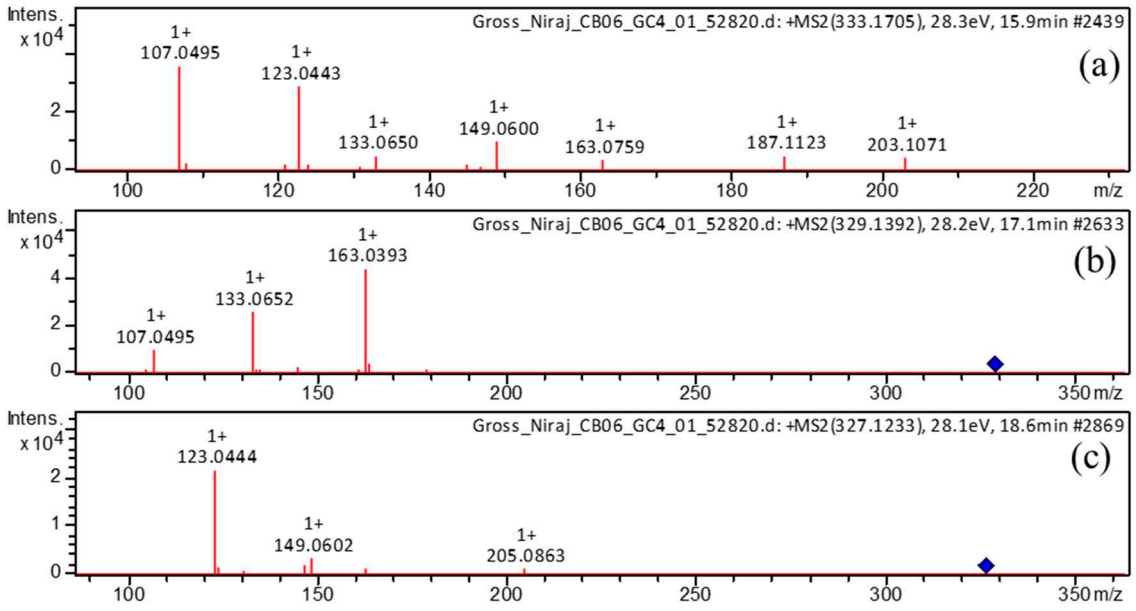

Figure 6. MS^2 profiles in (+)-ESI mode for: (a) Compound 4, (b) Compound 6, and (c) Compound 10.

Preprints (www.preprints.org) | NOT PEER-REVIEWED | Posted: 27 June 2023 doi:10.20944/preprints202306.1846.v1

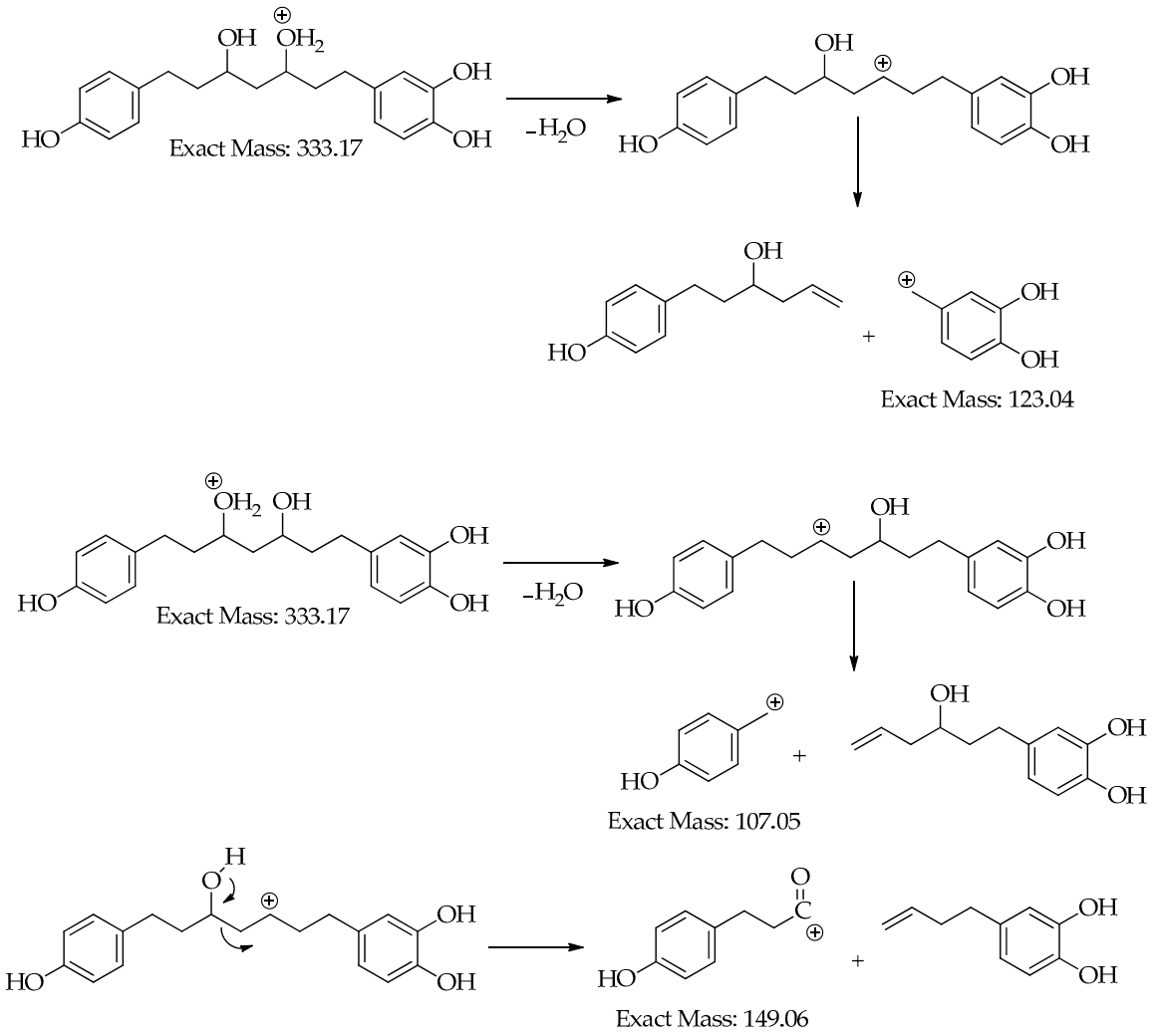

Figure 7. Observed fragmentation pattern of compound 4 in (+)-ESI mode.

Compound 5 eluted at 16.4 min showed a quasimolecular ion with *m/z* 329.1394 $[M-H]^-$. Its MS^2 profile (Figure 4b) showed a distinct base peak with *m/z* 135 because of the simultaneous removal of neutral unit $C_{11}H_{12}O_3$ and H_2 i.e. $[M-H-C_{11}H_{12}O_3-H_2]^-$. Based on fragment ions (Figure 8) formed, this compound was annotated as 5-hydroxy-1-(4-hydroxyphenyl)-7-(3,4-dihydroxyphenyl)-3-heptanone.

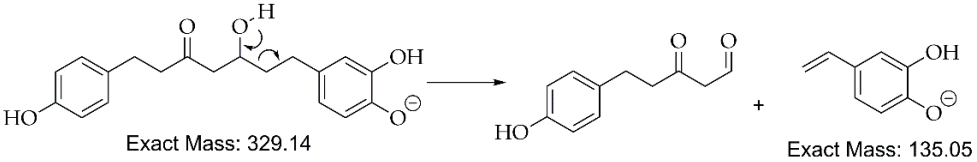

Figure 8. Observed fragmentation pattern of compound 5 in (–)-ESI mode.

Compound 6 was eluted at 17.1 minutes and it displayed a molecular ion with *m/z* 329.1392 $[M+H]^+$ and *m/z* 327.1239 $[M-H]^-$ in the(+)-ESI and (–)-ESI modes respectively. Its MS^2 profile (Figure 6b) in the (+)-ESI mode revealed a distinct base peak with *m/z* 163 $[M+H-166]^+$ resulting from the breakage of the $C_9H_{10}O_3$ unit. Further, a daughter ion with *m/z* 107 $[M+H-206-OH]^+$ was observed because of the elimination of the $C_{12}H_{14}O_3$ moiety followed by the –OH group. Hence, based on fragmentation behavior (Figure 9), this compound was identified as 1,7-bis(3,4-dihydroxyphenyl)hept-4-en-3-one.

Preprints (www.preprints.org) | NOT PEER-REVIEWED | Posted: 27 June 2023 doi:10.20944/preprints202306.1846.v1

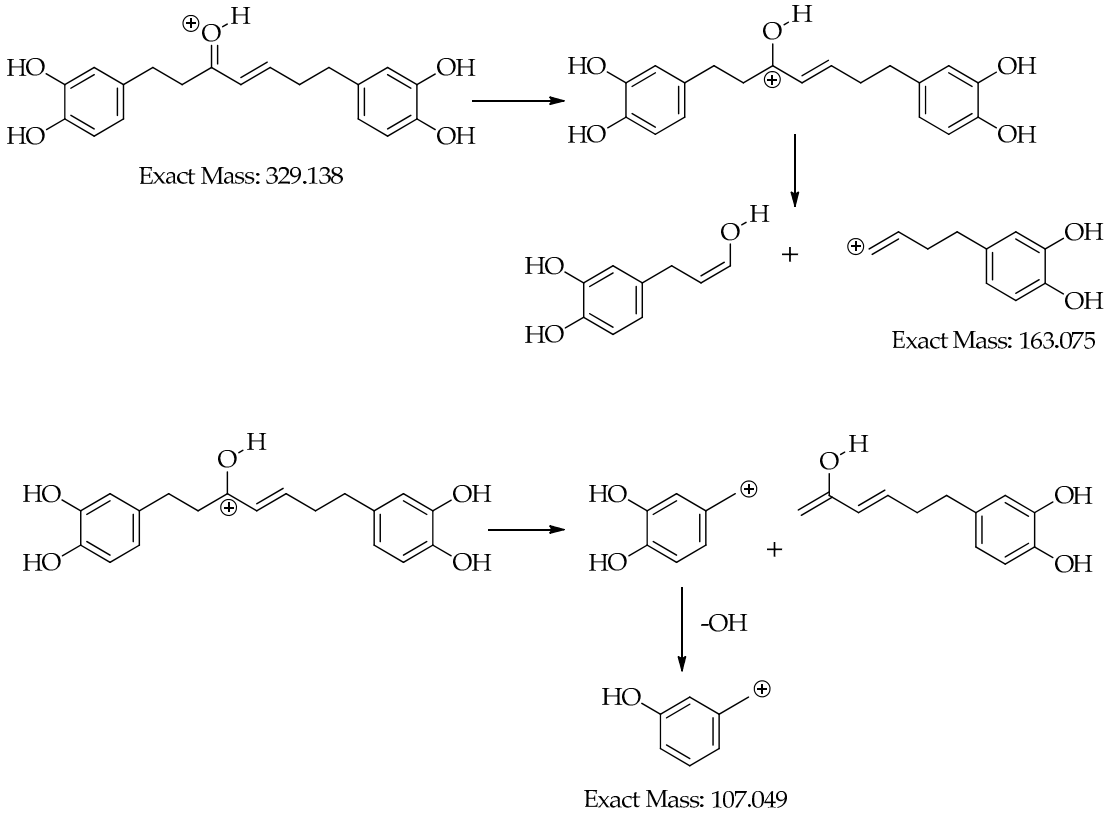

Figure 9. Observed fragmentation pattern of compound 6 in (+)-ESI mode.

Compound 10 eluted at 18.6 min showed molecular ions with *m/z* 327.1233 $[M+H]^+$ in the (+)-ionization and with *m/z* 325.1079 $[M-H]^-$ in (–)-ionization. The MS^2 spectrum in positive mode (Figure 6c) revealed a peak with *m/z* 123 $[M+H-204]^+$ as the base peak because of removal the of the neutral $C_{12}H_{12}O_3$ unit. Besides, fragments ions (Figure 10) are observed with *m/z* 205 $[M+H-122]^+$ because of the elimination of $C_7H_6O_2$, and *m/z* 189 $[M+H-138]^+$ attributed to the elimination of neutral $C_8H_{10}O_2$ unit. Similarly, its MS^2 profile in negative mode (Figure 4c) revealed a base peak with m/z 203 $[M-H-122]^-$ because of the loss of neutral unit $C_7H_6O_2$. Another minor peak was detected at m/z 135 because of the breakdown of the neutral $C_{11}H_{10}O_3$ unit. Based on fragment ions (Figure 11), this compound was identified as 1,7-bis(3,4-dihydroxyphenyl)hepta-4,6-dien-3-one.

Preprints (www.preprints.org) | NOT PEER-REVIEWED | Posted: 27 June 2023 doi:10.20944/preprints202306.1846.v1

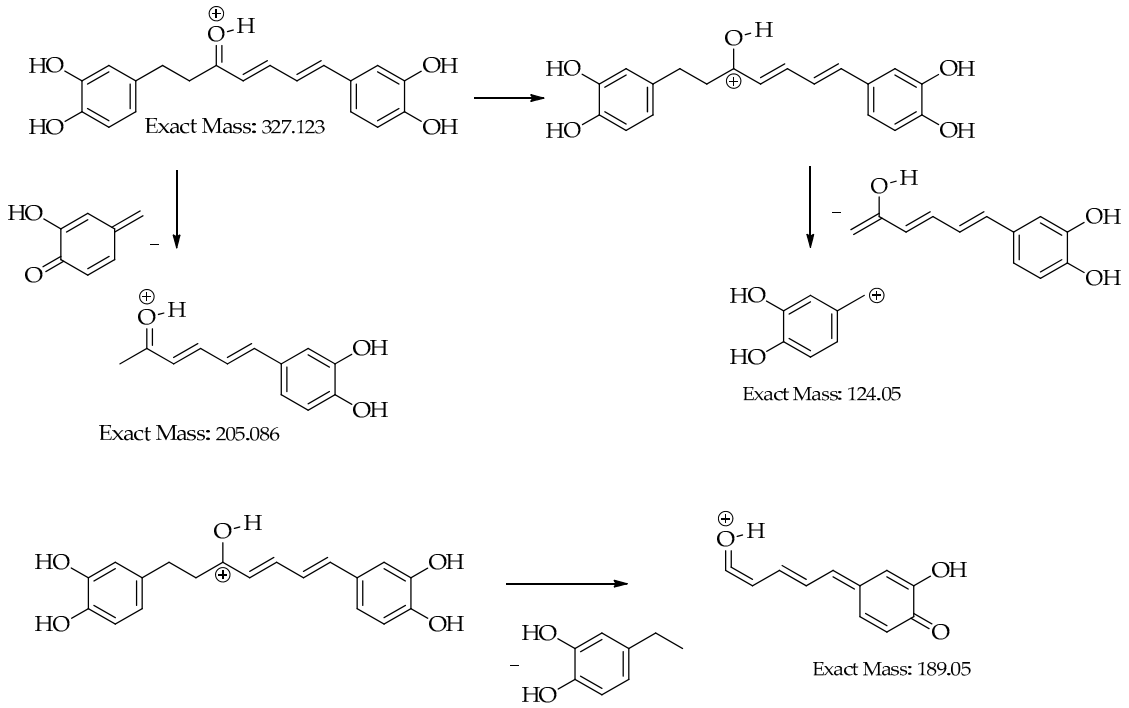

Figure 10. Observed fragmentation pattern of compound 10 in (+)-ESI mode.

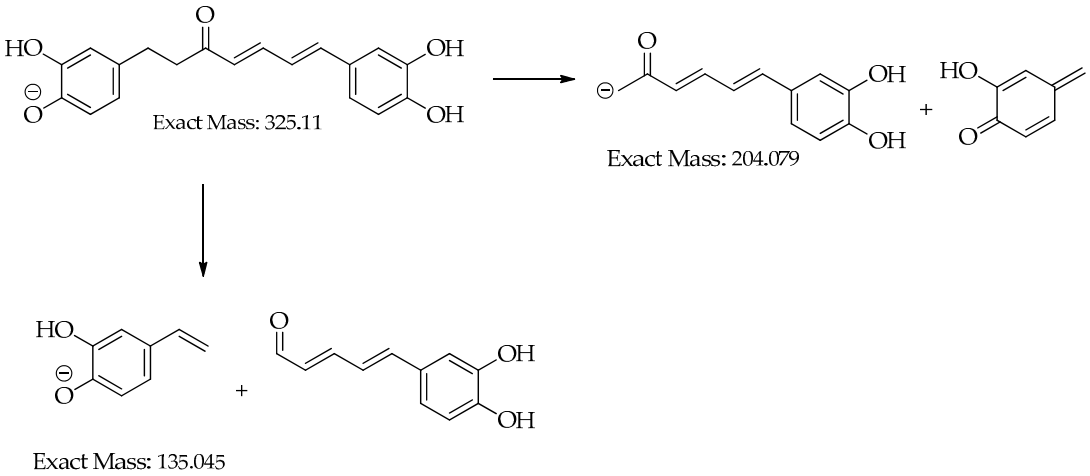

Figure 11. Observed fragmentation pattern of compound 10 in (–)- ESI mode.

3.3. GNPS-Based Molecular Networking

Molecular networking analysis is an analytical method to analyze and visualize metabolites from HR-MS/MS data. Within the molecular network, where each metabolite is depicted as a node with its corresponding *m*/*z* value. This network consists of multiple clusters based on the resemblance of molecular fragmentation patterns, which indicates that they share similar core chemical structures [30]. A total of 476 individual ions are observed as nodes and 576 as edges in the molecular network in which 3 clusters A, B, and C are formed as shown in Figure 12.

Preprints (www.preprints.org) | NOT PEER-REVIEWED | Posted: 27 June 2023 doi:10.20944/preprints202306.1846.v1

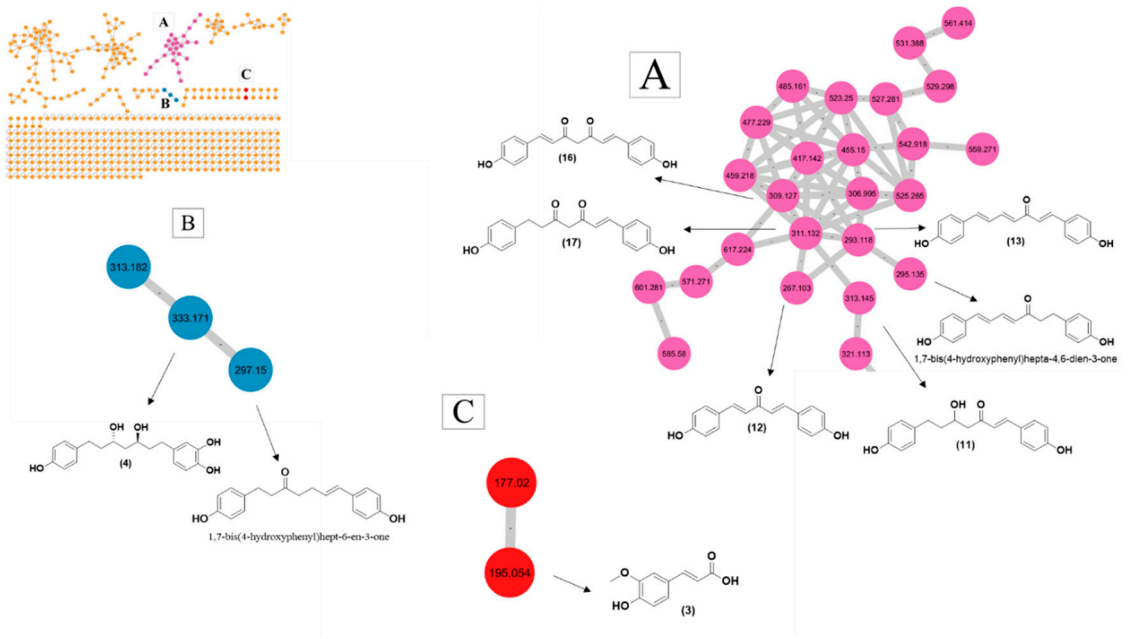

Figure 12. Molecular networking (Cluster A, B, and C) and identification of secondary metabolites from the *C. longa* L. rhizome extracts.

4. Discussion

4.1. Metabolite Profiling Based on MS¹ and MS² Spectra

Curcuma species are recognized for the abundantly presence of turmerones, sesquiterpenes, and, diarylheptanoids [31–33]. Diarylheptanoids, a class of compounds with remarkable biological effects, can be recognized by the 1,7-diphenylheptane framework and have recently attracted attention [34]. Compound 1, already reported in the leaves of *Alnus japonica*, was tentatively identified in *C. longa* L. rhizomes for the first time as 1,7-bis(3,4-dihydroxyphenyl)-5-hydroxyheptan-3-one [35]. Compound 4 was annotated as 3,5-dihydroxy-1-(3,4-dihydroxyphenyl)-7-(4-hydroxyphenyl)heptane. Although previously reported this compound from *C. kwangsiensis* [36], this is the first time it was observed in *C. longa* L. Compound 5 was putatively identified as 5-hydroxy-1-(4-hydroxyphenyl)-7-(3,4-dihydroxyphenyl)-3-heptanone. The presence of this compound was detected previously in the rhizomes of *C. kwangsiensis* [36], and it was observed for the first time in *C. longa* rhizomes. Compound 6 was tentatively identified as 1,7-bis(3,4-dihydroxyphenyl)hept-4-en-3-one, previously reported in the leaves of *Corylus maxima* [37], and its presence was detected for the first time in *C. longa.* This compound was reported to show an anti-inflammatory effect [38].

The molecular ion of compound 7 was detected at 17.4 min with *m/z* 315.1602 $[M-H]^-$. The MS^2 spectrum revealed a daughter ion with *m/z* 193 $[M-H-122]^-$ because of the elimination of ethylphenol $C_8H_{10}O$ unit. Moreover, the elimination of $C_{10}H_{14}O_2$ unit from the precursor ion gave a base peak at *m/z* 149 $[M-H-166]^-$ that further eliminate a CO molecule to give a daughter peak with *m/z* 121$[M-H-166-CO]^-$ followed by the departure of methyl radical so that a fragment was observed with *m/z* 106 $[M-H-166-CO-CH_3]^-$. Additionally, a daughter ion with *m/z* 163 [M-H-150-2]$^-$ attributed to the simultaneous elimination of the $C_9H_{10}O_2$ unit and H_2 was detected. Hence, compound 7 was recognized as 1,7-bis(4-hydroxyphenyl)-3,5-heptanediol, which was already reported in *C. longa* L. [39]. Compound 8 displayed

Preprints (www.preprints.org) | NOT PEER-REVIEWED | Posted: 27 June 2023 doi:10.20944/preprints202306.1846.v1

molecular ion with m/z 325.1082 $[M-H]^-$ at 17.7 min and its MS^2 profile showed characteristic fragments ion with *m/z* 307 $[M-H-H_2O]^-$ owing to the elimination of a water molecule, *m/z* 187 due to $[M-H-H_2O-C_7H_4O_2]^-$, *m/z* 161 attributed to $[M-H-C_9H_8O_3]^-$ which further loss –OH group to generate a base peak with *m/z* 145 $[M-H-C_9H_8O_3-OH]^-$ as shown in Supplementary Figure S31. Thus, compound 8 was annotated as 3-hydroxy-1,7-bis(4-hydroxyphenyl)-6-heptene-1,5-dione, which was already reported in *C. longa* L. [40].

Compound 9 eluted at 18.3 minutes was detected as a quasimolecular ion at *m/z* 325.1080 $[M+H]^+$. Its MS^2 profile exhibited a base peak with *m/z* 147 due to the removal of $C_{10}H_{10}O_3$ moiety $[M+H-C_{10}H_{10}O_3]^+$. Additionally, a daughter ion with *m/z* 163 owing to $[M+H-C_{10}H_{10}O_2]^+$ was detected. As a result, compound (9) was tentatively annotated as 1-(4-hydroxyphenyl)-7-(3,4-dihydroxyphenyl)-1,6-heptadiene-3,5-dione [40]. Compound 10 was tentatively identified as 1,7-bis(3,4-dihydroxyphenyl)hepta-4,6-dien-3-one, reported previously from the rhizomes of *Dioscorea nipponica*. Based on the information available in the literature, this compound was observed in *C. longa* for the first time. It has been reported that this compound has shown an anti-neuroinflammatory effect suppressing NO generation in murine microglia BV-2 cells with IC_{50} = 7.84 μM [41]. Compound 11 eluted at 18.7 min showed quasimolecular ions with *m/z* 313.1441 $[M+H]^+$ as well as *m/z* 311.128 $[M-H]^-$ in the (+)-ESI and (–)-ESI, respectively. Its MS^2 spectrum in (+)-ESI mode displayed distinct fragment ions with *m/z* 147 $[M+H-18-148]^+$ as a base peak because of the removal of a water molecule followed by elimination of neutral $C_{10}H_{12}O$ unit and *m/z* 107 $[M+H-18-188]^+$ attributed to the removal of a water molecule followed by loss of $C_{12}H_{12}O_2$. The base peak $C_9H_7O_2^+$ (*m/z* 147) further eliminates a CO molecule to give a peak at *m/z* 119 $[C_9H_7O_2-CO]^+$. In a similar way, the MS^2 spectrum in (–)-ESI mode revealed a distinct base peak with *m/z* 161 $[M-H-150]^-$ attributed to the elimination of the $C_9H_{10}O_2$ unit. Additionally, fragments peak with *m/z* 149 corresponding to $[M-H-C_{10}H_{10}O_2]^-$ and *m/z* 119 because of $[M-H-C_{11}H_{12}O_3]^-$ were detected. Thus, compound 11 was annotated as 5-hydroxy-1,7-bis(4-hydroxyphenyl)hept-1-en-3-one, which was already reported in *C. longa* [39].

Compound 12 eluted at 20.6 min was detected as a quasimolecular ion with *m/z* 267.1021 $[M+H]^+$. Its MS^2 spectrum revealed a distinct base peak with *m/z* 147 $[M+H-120]^+$ corresponding to the elimination of the C_8H_8O unit. Besides, daughter ion with *m/z* 119 $[M+H-148]^+$ owing to elimination of $C_9H_8O_2$ unit, *m/z* 107 $[M+H-160]^+$ due to removal of $C_{10}H_8O_2$. Hence, compound 12 was tentatively annotated as 1,5-bis(4-hydroxyphenyl)-1,4-pentadiene-3-one, formerly reported in *Curcuma domestica* [42]. Compound 13 showed molecular ions with *m/z* 293.1178 $[M+H]^+$ in positive ionization at 22.4 min and *m/z* 291.1029 $[M-H]^-$ in (–)-ESI ionization at 22.2 min. The MS^2 profile in negative mode revealed characteristic peaks at *m/z* 171 as base peaks owing to $[M-H-C_8H_8O]^-$, *m/z* 145 because of $[M-H-C_9H_6O_2]^-$ ion and *m/z* 119 owing to $[M-H-C_{11}H_8]^-$. Thus, compound 13 was tentatively detected as 1,7-bis(4-hydroxyphenyl)hepta-1,4,6-trien-3-one, previously reported in *C. longa* [43]. Compound 14 was detected in negative ionization mode at 22.4 min with quasimolecular ion with *m/z* 323.0928 $[M-H]^-$. Its MS^2 spectrum revealed a base peak with *m/z* 135 $[M-H-188]^-$ with the elimination of $C_{11}H_8O_3$. Apart from this, fragments peak with *m/z* 119 $[M-H-204]^-$ was detected with the elimination of $C_{11}H_8O_4$. Thus,

Preprints (www.preprints.org) | NOT PEER-REVIEWED | Posted: 27 June 2023 doi:10.20944/preprints202306.1846.v1

the compound was identified as 1-(3,4-dihydroxyphenyl)-7-(4-hydroxyphenyl)hepta-1,6-diene-3,5-dione, which was already reported in *C. longa* [40]. Compound 15 was detected at 22.4 and 22.8 min with quasimolecular ions with *m/z* 355.1185 $[M+H]^+$ and *m/z* 353.1034 $[M-H]^-$ in (+)- ESI and (–)-ESI ionization respectively. Its MS^2 profile revealed a distinctive peak with *m/z* 271, which corresponds to daughter ion $[M+H-84]^+$ after the elimination of $C_4H_4O_2$. Likewise, fragments peak with *m/z* 177 $[M+H-178]^+$ after the elimination of $C_{10}H_{10}O_3$, and *m/z* 163 $[M+H-192]^+$ after the removal of $C_{11}H_{12}O_3$. Thus, compound 15 was identified as monodemethylcurcumin, which was already reported in *C. domestica* [44].

Compound 16 has molecular ion at *m/z* 309.1127 in (+)-ESI ionization and *m/z* 307.0979 in (–)-ESI ionization, and was identified as bisdemethoxycurcumin, which was previously observed in *C. longa* [45]. Its MS^2 profile in positive mode revealed a distinctive peak with *m/z* 147 $[M+H-162]^+$ as the base peak corresponding to the elimination of the $C_{10}H_{10}O_2$ unit. A daughter ion was observed at *m/z* 225 $[M+H-84]^+$ attributed to break down of the $C_4H_4O_2$ unit, which further eliminate a phenol molecule to give a peak at *m/z* 131 $[M+H-C_4H_4O_2-C_6H_6O]^+$. Additionally, another daughter ion was observed with *m/z* 107 $[M+H-205]^+$ because of the breakage of the $C_{12}H_{13}O_3$ unit. The observed fragmentation pattern of compound 16 is shown in supplementary Figure S32. Compound 17 displayed molecular ions with *m/z* 311.1280 $[M+H]^+$ and *m/z* 309.1132 $[M-H]^-$, at 24.2 min. Its MS^2 profile revealed a distinct peak with *m/z* 147 $[M+H-164]^+$ as a base peak because of the elimination of $C_{10}H_{12}O_2$. Besides this, distinct peaks at *m/z* 107 attributed to $[M+H-C_{12}H_{12}O_3]^+$, *m/z* 225 owing to $[M+H-C_4H_4O_2]^+$, and *m/z* 131 $[M+H-C_4H_4O_2-C_6H_6O]^+$ corresponding to an elimination of a phenol molecule from *m/z* 225. Thus, compound 17 was identified as 1,7-bis(4-hydroxyphenyl)hept-1-ene-3,5-dione, and this compound was already reported in *C. longa* L. [43]. The observed fragmentation pattern of compound 17 is shown in Figure S33. Compound 18 exhibited molecular ions with *m/z* 339.1229 $[M+H]^+$ in (+)-ESI mode at 24.8 min and *m/z* 337.1085 $[M-H]^-$ in (–)-ESI mode at 25.0 min. Its MS^2 profile in positive mode revealed characteristic peaks with *m/z* 177 because of $[M+H-C_{10}H_{10}O_2]^+$ as base peak, *m/z* 147 resulting from $[M+H-C_{11}H_{12}O_3]^+$ and, *m/z* 255 owing to $[M+H-C_4H_4O_2]^+$. Thus, compound 18 was tentatively identified as demethoxycurcumin and it was previously reported in *C. longa* L [40,43]. The observed fragmentation pattern of this compound is shown in Figure S34. Compound 19 displayed molecular ions with *m/z* 369.1337 $[M+H]^+$ and *m/z* 367.1190 $[M-H]^-$ at 25.3 min in (+)-ESI and (–)-ESI mode respectively. Its MS^2 spectrum displayed a distinctive base peak with *m/z* 177 $[M+H-192]^+$ owing to the breakdown of the $C_{11}H_{12}O_3$ unit. Additionally, typical fragments with *m/z* 285 because of $[M+H-C_4H_4O_2]^+$ and *m/z* 161 corresponding to the elimination of the $C_7H_8O_2$ unit from *m/z* 285 were observed. Thus, compound 19 was identified as curcumin and which is the most abundant curcuminoid reported in *C. longa* L [43,46]. The observed fragmentation pattern of curcumin is shown in Figure S35.

Compound 20 displayed a quasimolecular ion with *m/z* 543.2747 $[M+H]^+$ at 27.0 min in positive ionization mode. The MS^2 spectrum revealed a peak with *m/z* 147 as the base peak because of $[M+H-C_{25}H_{32}O_4]^+$, *m/z* 309 $[M+H-C_{15}H_{24}O_2]^+$ owing to the breakage of bisabolene unit. Hence, compound 20 was putatively annotated as didemethoxybisabolocurcumin ether and this compound was previously observed

in *C. longa* L [47]. Additionally, compounds 21 and 22 displayed sodium adduct ion peaks at *m/z* 595.2675 $[M+Na]^+$ and *m/z* 625.2786 $[M+Na]^+$ at 30.1 and 30.7 min respectively, and compounds were tentatively identified as demethoxybisabolocurcumin ether and bisabolocurcumin ether respectively, based on the literature survey [47]. These three bisabolocurcumin ethers 20, 21, and 22 are the derivatives of curcuminoids. These compounds consist of a carbon-oxygen bond linking a bisabolene-type sesquiterpene substructure to a 1,7-diarylheptanoid framework.

Compound 2 eluted at 15.3 min was detected as quasimolecular ions with *m/z* 165.0551 $[M+H]^+$ and *m/z* 163.0401 $[M-H]^-$ in (+)-ESI and (–)-ESI modes respectively. Its MS^2 profile in positive mode showed fragments ion with *m/z* 147 $C_9H_9O_2^+$ because of the removal of water $[M+H-H_2O]^+$, which further loss CO molecule to generate base peak with *m/z* 119 $[M+H-H_2O-CO]^+$. The ion $C_8H_7O^+$ responsible for the base peak further loses CO molecule to give a daughter ion having *m/z* 91. Similarly, the MS^2 profile in negative mode revealed a characteristic peak with m/z 119 $[M-H-44]^-$ attributed to the removal of the CO_2 molecule, which further eliminated ethyne to generate daughter ion with *m/z* 93 $[M-H-CO_2-C_2H_2]^-$. Thus, compound 2 was annotated as 4-hydroxycinnamic acid which was already observed in *C. longa* L. [48]. Compound 3 showed quasimolecular ion with *m/z* 195.0657 $[M+H]^+$. Its MS^2 profile revealed characteristics fragments with *m/z* 177 because of $[M+H-H_2O]^+$, *m/z* 163 owing to $[M+H-CH_3OH]^+$ which further loss CO moiety to give a base peak at *m/z* 145. Thus, compound 3 was annotated as ferulic acid, which was reported previously in *C. longa* L. [48]. Compound 23 eluted at 16.0 min showed molecular ions with *m/z* 153.0547$[M+H]^+$ and *m/z* 151.0339 $[M-H]^-$. Its MS^2 profile in positive mode revealed a daughter ion with *m/z* 125 $[M+H-CO]^+$ because of the elimination of a CO molecule, which further lost a CH_3OH molecule to give a base peak with *m/z* 93. Further elimination of the CO molecule from *m/z* 93 generates a peak with *m/z* 65 $[M+H-CO-CH_3OH-CO]^+$. Moreover, its MS^2 profile in negative ion mode showed a base peak at *m/z* 136 $[M-H-CH_3]^-$ attributed to the removal of methyl radical that either eliminate CO moiety to give a peak at m/z 108 or loses a CO_2 molecule to give a peak at *m/z* 92. Thus, compound 23 was annotated as vanillin, previously reported in the rhizomes of *C. longa* L.[48].

Compound 24 was observed as a molecular ion with *m/z* 191.0712 $[M-H]^-$. Its MS^2 spectrum displayed a distinct base peak with *m/z* 176 $[M-H-CH_3]^-$ resulting from the breakdown of methyl radical. Thus, compound 24 was identified as dehydrozingerone, previously reported in *Zingiber officinale* [49]. Moreover, compound 25 was detected with *m/z* 235.1688 $[M+H]^+$ as a molecular ion in positive ionization mode. The MS^2 profile revealed fragment ion at *m/z* 161,*m/z* 135,*m/z* 121,*m/z* 119 (base peak), *m/z* 107, *m/z* 105, *m/z* 93 and *m/z* 83. This compound was annotated as dehydrocurdione and already reported in *C. longa* L [32]. Compound 28 eluted at 28.5 min displayed as quasimolecular ions with *m/z* 233.1534 $[M+H]^+$. The MS^2 spectrum revealed fragments at *m/z* 145, *m/z* 135, *m/z* 131 *m/z*, 120, *m/z* 119 (base peak), *m/z* 117, *m/z* 91, and *m/z* 83. This compound was annotated as turmeronol A and was already identified in the rhizome of *C. longa* [50]. Compound 30 was eluted at 31.2 min and showed a quasimolecular ion with m/z 217.1588 $[M+H]^+$. Its MS^2 profile revealed a base peak with *m/z* 119 $[M+H-98]^+$ because of the

 doi:10.20944/preprints202306.1846.v1

breakage of the $C_6H_{10}O$ unit. Hence, compound 30 was tentatively assigned as arturmerone and which was already observed in *C. zedoaria* [51].

Compound 26 displayed a molecular ion (at 26.4 min) with *m/z* 235.1697 $[M+H]^+$. The MS^2 spectrum showed fragment ions at *m/z* 213, *m/z* 198, *m/z* 175, *m/z* 147, *m/z* 133 (base peak), *m/z* 107 and *m/z* 97. Therefore, compound 26 was tentatively annotated as (6s)-6-methyl-5-(3-oxobutyl)-2-(propan-2-ylidene)cyclohept-4-en-1-one and it was previously reported in *C. aromatica* [52]. Compound 27 was eluted at 28.0 min and it displayed a molecular ion with *m/z* 293.2125. Its MS^2 spectrum exhibited daughter ions at *m/z* 275 (base peak), *m/z* 235, *m/z* 231, *m/z* 232, *m/z* 171, and *m/z* 121. Therefore, compound 27 was putatively identified as 9-hydroxy-10, 12, 15-octadecatrienoic acid which was already reported in the leaf of *Isatis tinctoria* [53]. Compound 29 eluted at 29.6 min and exhibited a molecular ion with *m/z* 295.2282 $[M-H]^-$. Its MS^2 spectrum revealed daughter ions with *m/z* 277 (base peak), *m/z* 195, *m/z* 183, and *m/z* 171. Hence, compound 29 was tentatively annotated as coriolic acid which was previously reported in *Deprea subtriflora* [54].

Similarly, precursor ions eluted at a retention time of 19.3 min with *m/z* 353.1024, and *m/z* 383.1132 at a retention time of 19.5 min in the positive mode of ionization of ethyl acetate fraction were not further analyzed because these precursor ions have not undergone fragmentation. Further, due to the low abundance of some metabolites in ethyl acetate fraction, these could not exhibit intense peaks in the base peak chromatogram (Figure 1).

4.2. GNPS-Based Metabolite Profiling

A large cluster A formed in molecular networking (Figure 12) characterized by precursor ions with *m/z* 309.127, *m/z* 311.132, *m/z* 267.103, *m/z* 313.145, and *m/z* 293.118 were identified as compounds 16, 17, 12, 11, 13, respectively, which were previously identified on manual annotation. In cluster A, a precursor ion with *m/z* 295.135 shows similarity in MS^2 spectra with *m/z* 293.118 and has a mass difference of only 2 Da. This showed that there should be one double bond difference between these precursor ions. Thus, precursor ion *m/z* 295.135 was identified as 1,7-bis(4-hydroxyphenyl)hepta-4,6-dien-3-one, isolated and reported previously from the rhizomes of *C. kwangsiensis* [55]. Moreover, another small cluster B consisting of 3 precursor ions (*m/z* 333.171, *m/z* 297.150, and *m/z* 313.182), ion *m/z* 333.171 identified as 3,5-dihydroxy-1-(3,4-dihydroxyphenyl)-7-(4-hydroxyphenyl)heptane. The neutral loss of 36.021 Da from precursor ion at m/z 333.171 and the cosine value of 0.8827 suggest precursor ion *m/z* 297.150 have similarity in MS^2 spectra with *m/z* 333.171. Thus, the precursor ion at *m/z* 297.150 was putatively identified as 1,7-bis(4-hydroxyphenyl)hept-6-ene-3-one. Additional research is required to explore the unidentified nodes and edges present in the molecular networking, as the majority of the metabolites detected in this research were already reported in *C. longa* L.

In this research, most of the metabolites detected are non-volatile, polar molecules since the LC-HR-ESI-MS/MS-based analysis is limited to the detection of compounds with heteroatoms. As a result, therapeutically valued volatile compounds found in the *C. longa* rhizomes may be excluded by this approach and

GC-MS-based analysis may become a choice for the detection of such compounds. Some of the metabolites were detected in hexane fraction despite their polarity. This may be due to incomplete fractionation of rhizomes extracts.

Moreover, most of the diarylheptanoids were detected in the negative ion mode. The reason why diarylheptanoids are appropriate for detection in negative ion mode is that they contain multiple hydroxyl groups. These hydroxyl groups make it effortless for the ionization in negative mode. Moreover, diarylheptanoids with low abundance were easily detected in the positive ionization mode but not in the negative ionization mode. This observation indicates the low sensitivity of the negative mode in comparison to the positive mode of ionization. Additionally, it was found that the absence of a keto group in the heptyl chain affected the protonation of low abundance diarylheptanoids in positive ion mode and imposed difficulty for the fragmentation in negative ion modes, as mentioned previously [39].

5. Conclusions

Turmeric has been widely used in food as spices and herbal medication and is a rich source of therapeutically active compounds. We chose liquid chromatography coupled with mass spectrometry owing to its high sensitivity and selectivity. This hyphenated technique is gaining popularity in the past two decades in metabolomics studies to explore, identify, and validate naturally occurring bioactive compounds as well as biomarkers in the medicinal field. We used HPLC-HR-ESI-MS/MS-based metabolomics approach along with molecular networking to study the metabolites in the turmeric extracts. The metabolic profiling of ethyl acetate and hexane fractions in both ionization modes showed the presence of 30 annotated metabolites including 16 diarylheptanoids, 1 diarylpentanoid, 4 sesquiterpenoids, 3 bisabolocurcumin derivatives, 4 cinnamic acid derivatives, and 2 fatty acid derivatives. Five diarylheptanoids were identified for the first time in the *C. longa* L. rhizomes. We have initiated this project where we analyzed the overall metabolome of *C. longa* L. In the future, we plan to work with several other traditionally important species to discover the differences in metabolite profile and evaluate their bioactivities. Additional research is recommended to isolate and validate newly identified diarylheptanoid compounds and explore compounds in different *Curcuma* species and check their bioactivities through *in silico*, *in vitro*, and *in vivo* experiments to develop potential drug candidates and food supplements.

Supplementary Materials: The following supporting information can be downloaded at the website of this paper posted on Preprints.org., Figure S1: MS^1 and MS^2 spectra of compound 1, Figure S2: MS^1 and MS^2 spectra of compound 2, Figure S3: MS^1 and MS^2 spectra of compound 3, Figure S4: MS^1 and MS^2 spectra of compound 4, Figure S5: MS^1 and MS^2 spectra of compound 5, Figure S6: MS^1 and MS^2 spectra of compound 6, Figure S7: MS^1 and MS^2 spectra of compound 7, Figure S8: MS^1 and MS^2 spectra of compound 8, Figure S9: MS^1 and MS^2 spectra of compound 9, Figure S10: MS^1 and MS^2 spectra of compound 10, Figure S11: MS^1 and MS^2 spectra of compound 11, Figure S12: MS^1 and MS^2 spectra of compound 12, Figure S13: MS^1 and MS^2 spectra of compound 13, Figure S14: MS^1 and MS^2 spectra of compound 14, Figure S15: MS^1 and MS^2 spectra of compound 15, Figure S16: MS^1 and MS^2 spectra of compound 16, Figure S17: MS^1 and MS^2 spectra of compound 17, Figure S18: MS^1 and MS^2 spectra of compound 18, Figure S19: MS^1 and MS^2 spectra of compound 19, Figure S20: MS^1 and MS^2 spectra of compound 20, Figure S21: MS^1 and MS^2 spectra of compound 21, Figure S22: MS^1 and MS^2 spectra of compound 22, Figure S23: MS^1 and MS^2 spectra of compound 23, Figure S24: MS^1 and MS^2 spectra of compound 24, Figure S25: MS^1 and MS^2 spectra of compound 25, Figure S26: MS^1 and MS^2 spectra of compound 26, Figure S27: MS^1 and MS^2 spectra of compound 27, Figure S28: MS^1 and MS^2 spectra of compound 28, Figure S29: MS^1 and MS^2

spectra of compound 29, Figure S30: MS^1 and MS^2 spectra of compound 30, Figure S31: Observed fragmentation pattern of compound 8 in (–)-ESI mode, Figure S32: Observed fragmentation pattern of compound 16 in (+)-ESI mode, Figure S33: Observed fragmentation pattern of compound 17 in (+)-ESI mode, Figure S34: Observed fragmentation pattern of compound 18 in (+)-ESI mode, and Figure S35: Observed fragmentation pattern of compound 19 in (+)-ESI mode.

Author Contributions: Conceptualization, N.A. and N.P.; methodology, R.B., and A.P.T.; software, R.B., A.P.T., and N.A.; validation, N.P. B.P.R. and K.R.S.; formal analysis, N.A.; writing—original draft preparation, R.B. and A.P.T; writing—review and editing, N.A., B.P.R., and K.R.S.; supervision, N.P., B.P.R, and K.R.S.; project administration, N.P.; funding acquisition, N.P. All authors have read and agreed to the published version of the manuscript.

Funding: This research was funded by the University Grants Commission (Nepal), Grant number: CRIG-78/79-S&T-01 (to N.P.).

Institutional Review Board Statement: Not applicable.

Informed Consent Statement: Not applicable.

Data Availability Statement: Data are reported in the article and the Supplementary Materials or are available from the corresponding authors upon reasonable request.

Acknowledgments: Authors would like to acknowledge Gross lab, the University of Tubingen, Germany for the measurement of LC-HRMS data.

Conflicts of Interest: The authors declare no conflict of interest.

References

1. Rathaur, P. Turmeric : The Golden Spice Of Life. **2012**.
2. Issuriya, A.; Kumarnsit, E.; Wattanapiromsakul, C.; Vongvatcharanon, U. Histological Studies of Neuroprotective Effects of Curcuma Longa Linn. on Neuronal Loss Induced by Dexamethasone Treatment in the Rat Hippocampus. *Acta Histochemica* **2014**, *116*, 1443–1453, doi:10.1016/j.acthis.2014.09.009.
3. Oliveira, G.; Marques, C.; de Oliveira, A.; de Almeida dos Santos, A.; do Amaral, W.; Ineu, R.P.; Leimann, F.V.; Peron, A.P.; Igarashi-Mafra, L.; Mafra, M.R. Extraction of Bioactive Compounds from Curcuma Longa L. Using Deep Eutectic Solvents: In Vitro and in Vivo Biological Activities. *Innovative Food Science & Emerging Technologies* **2021**, *70*, 102697, doi:10.1016/j.ifset.2021.102697.
4. Araújo, C. a. C.; Leon, L.L. Biological Activities of Curcuma Longa L. *Mem. Inst. Oswaldo Cruz* **2001**, *96*, 723–728, doi:10.1590/S0074-02762001000500026.
5. Sun, D.-J.; Zhu, L.-J.; Zhao, Y.-Q.; Zhen, Y.-Q.; Zhang, L.; Lin, C.-C.; Chen, L.-X. Diarylheptanoid: A Privileged Structure in Drug Discovery. *Fitoterapia* **2020**, *142*, 104490, doi:10.1016/j.fitote.2020.104490.
6. Jayaprakasha, G.K.; Jaganmohan Rao, L.; Sakariah, K.K. Antioxidant Activities of Curcumin, Demethoxycurcumin and Bisdemethoxycurcumin. *Food Chemistry* **2006**, *98*, 720–724, doi:10.1016/j.foodchem.2005.06.037.
7. de Oliveira Filho, J.G.; de Almeida, M.J.; Sousa, T.L.; dos Santos, D.C.; Egea, M.B. Bioactive Compounds of Turmeric (Curcuma Longa L.). In *Bioactive Compounds in Underutilized Vegetables and Legumes*; Murthy, H.N., Paek, K.Y., Eds.; Reference Series in Phytochemistry; Springer International Publishing: Cham, 2021; pp. 297–318 ISBN 978-3-030-57415-4.
8. Tayyem, R.F.; Heath, D.D.; Al-Delaimy, W.K.; Rock, C.L. Curcumin Content of Turmeric and Curry Powders. *Nutrition and Cancer* **2006**, *55*, 126–131, doi:10.1207/s15327914nc5502_2.
9. Li, Y.; Kong, D.; Fu, Y.; Sussman, M.R.; Wu, H. The Effect of Developmental and Environmental Factors on Secondary Metabolites in Medicinal Plants. *Plant Physiology and Biochemistry* **2020**, *148*, 80–89, doi:10.1016/j.plaphy.2020.01.006.
10. Shulaev, V. Metabolomics Technology and Bioinformatics. *Briefings in Bioinformatics* **2006**, *7*, 128–139, doi:10.1093/bib/bbl012.
11. Dunn, W.B.; Bailey, N.J.C.; Johnson, H.E. Measuring the Metabolome: Current Analytical Technologies. *Analyst* **2005**, *130*, 606–625, doi:10.1039/B418288J.
12. Dettmer, K.; Aronov, P.A.; Hammock, B.D. Mass Spectrometry-Based Metabolomics. *Mass Spectrometry Reviews* **2007**, *26*, 51–78, doi:10.1002/mas.20108.
13. Zhang, X.; Li, Q.; Xu, Z.; Dou, J. Mass Spectrometry-Based Metabolomics in Health and Medical Science: A Systematic Review. *RSC Adv.* **2020**, *10*, 3092–3104, doi:10.1039/C9RA08985C.

14. Vincenti, F.; Montesano, C.; Di Ottavio, F.; Gregori, A.; Compagnone, D.; Sergi, M.; Dorrestein, P. Molecular Networking: A Useful Tool for the Identification of New Psychoactive Substances in Seizures by LC–HRMS. *Frontiers in Chemistry* **2020**, *8*.
15. Saleem, A.; Husheem, M.; Härkönen, P.; Pihlaja, K. Inhibition of Cancer Cell Growth by Crude Extract and the Phenolics of Terminalia Chebula Retz. Fruit. *Journal of Ethnopharmacology* **2002**, *81*, 327–336, doi:10.1016/S0378-8741(02)00099-5.
16. Li, L.; Yu, Y.; Lu, D.; Chen, J.; Guo, J.; Liang, J.; Zhang, A.; Yang, Z. Bioassay-Guided Separation and Identification of the Anticancer Composition from Curcuma Longa L. by the Combination Strategy of Methanol Gradient Countercurrent Chromatography and Ultra-High-Performance Liquid Chromatography Coupled with High-Resolution Mass Spectrometry. *Journal of Separation Science* **2022**, *45*, 4478–4490, doi:10.1002/jssc.202200348.
17. Segneanu, A.-E.; Vlase, G.; Lukinich-Gruia, A.T.; Herea, D.-D.; Grozescu, I. Untargeted Metabolomic Approach of Curcuma Longa to Neurodegenerative Phytocarrier System Based on Silver Nanoparticles. *Antioxidants* **2022**, *11*, 2261, doi:10.3390/antiox11112261.
18. Okuda-Hanafusa, C.; Uchio, R.; Fuwa, A.; Kawasaki, K.; Muroyama, K.; Yamamoto, Y.; Murosaki, S. Turmeronol A and Turmeronol B from Curcuma Longa Prevent Inflammatory Mediator Production by Lipopolysaccharide-Stimulated RAW264.7 Macrophages, Partially via Reduced NF-KB Signaling. *Food Funct.* **2019**, *10*, 5779–5788, doi:10.1039/C9FO00336C.
19. Guo, Y.-Q.; Wu, G.-X.; Peng, C.; Fan, Y.-Q.; Li, L.; Liu, F.; Xiong, L. New Bisabolane-Type Sesquiterpenoids from Curcuma Longa and Their Anti-Atherosclerotic Activity. *Molecules* **2023**, *28*, 2704, doi:10.3390/molecules28062704.
20. Lin, X.; Ji, S.; Li, R.; Dong, Y.; Qiao, X.; Hu, H.; Yang, W.; Guo, D.; Tu, P.; Ye, M. Terpecurcumins A–I from the Rhizomes of Curcuma Longa: Absolute Configuration and Cytotoxic Activity. *J. Nat. Prod.* **2012**, *75*, 2121–2131, doi:10.1021/np300551g.
21. Dong, S.; Luo, X.; Liu, Y.; Zhang, M.; Li, B.; Dai, W. Diarylheptanoids from the Root of Curcuma Aromatica and Their Antioxidative Effects. *Phytochemistry Letters* **2018**, *27*, 148–153, doi:10.1016/j.phytol.2018.07.021.
22. Quirós-Fallas, M.I.; Vargas-Huertas, F.; Quesada-Mora, S.; Azofeifa-Cordero, G.; Wilhelm-Romero, K.; Vásquez-Castro, F.; Alvarado-Corella, D.; Sánchez-Kopper, A.; Navarro-Hoyos, M. Polyphenolic HRMS Characterization, Contents and Antioxidant Activity of Curcuma Longa Rhizomes from Costa Rica. *Antioxidants* **2022**, *11*, 620, doi:10.3390/antiox11040620.
23. Ye, Y.; Zhang, X.; Chen, X.; Xu, Y.; Liu, J.; Tan, J.; Li, W.; Tembrock, L.R.; Wu, Z.; Zhu, G. The Use of Widely Targeted Metabolomics Profiling to Quantify Differences in Medicinally Important Compounds from Five Curcuma (Zingiberaceae) Species. *Industrial Crops and Products* **2022**, *175*, 114289, doi:10.1016/j.indcrop.2021.114289.
24. Wang, M.; Carver, J.J.; Phelan, V.V.; Sanchez, L.M.; Garg, N.; Peng, Y.; Nguyen, D.D.; Watrous, J.; Kapono, C.A.; Luzzatto-Knaan, T.; et al. Sharing and Community Curation of Mass Spectrometry Data with Global Natural Products Social Molecular Networking. *Nat Biotechnol* **2016**, *34*, 828–837, doi:10.1038/nbt.3597.
25. Aryal, N.; Chen, J.; Bhattarai, K.; Hennrich, O.; Handayani, I.; Kramer, M.; Straetener, J.; Wommer, T.; Berscheid, A.; Peter, S.; et al. High Plasticity of the Amicetin Biosynthetic Pathway in Streptomyces Sp. SHP 22-7 Led to the Discovery of Streptcytosine P and Cytosaminomycins F and G and Facilitated the Production of 12F-Plicacetin. *Journal of Natural Products* **2022**, doi:10.1021/acs.jnatprod.1c01051.
26. Dührkop, K.; Fleischauer, M.; Ludwig, M.; Aksenov, A.A.; Melnik, A.V.; Meusel, M.; Dorrestein, P.C.; Rousu, J.; Böcker, S. SIRIUS 4: A Rapid Tool for Turning Tandem Mass Spectra into Metabolite Structure Information. *Nat Methods* **2019**, *16*, 299–302, doi:10.1038/s41592-019-0344-8.
27. PubChem PubChem Available online: https://pubchem.ncbi.nlm.nih.gov/ (accessed on 30 May 2023).
28. Rutz, A.; Sorokina, M.; Galgonek, J.; Mietchen, D.; Willighagen, E.; Gaudry, A.; Graham, J.G.; Stephan, R.; Page, R.; Vondrášek, J.; et al. The LOTUS Initiative for Open Knowledge Management in Natural Products Research. *eLife* **2022**, *11*, e70780, doi:10.7554/eLife.70780.
29. ChemSpider | Search and Share Chemistry Available online: http://www.chemspider.com/ (accessed on 26 June 2023).
30. Quinn, R.A.; Nothias, L.-F.; Vining, O.; Meehan, M.; Esquenazi, E.; Dorrestein, P.C. Molecular Networking As a Drug Discovery, Drug Metabolism, and Precision Medicine Strategy. *Trends in Pharmacological Sciences* **2017**, *38*, 143–154, doi:10.1016/j.tips.2016.10.011.

31. Ganapathy, G.; Preethi, R.; Moses, J.A.; Anandharamakrishnan, C. Diarylheptanoids as Nutraceutical: A Review. *Biocatal Agric Biotechnol* **2019**, *19*, 101109, doi:10.1016/j.bcab.2019.101109.
32. Ohshiro, M.; Kuroyanagi, M.; Ueno, A. Structures of Sesquiterpenes from Curcuma Longa. *Phytochemistry* **1990**, *29*, 2201–2205, doi:10.1016/0031-9422(90)83038-3.
33. Chao, I.-C.; Wang, C.-M.; Li, S.-P.; Lin, L.-G.; Ye, W.-C.; Zhang, Q.-W. Simultaneous Quantification of Three Curcuminoids and Three Volatile Components of Curcuma Longa Using Pressurized Liquid Extraction and High-Performance Liquid Chromatography. *Molecules* **2018**, *23*, 1568, doi:10.3390/molecules23071568.
34. Alberti, Á.; Riethmüller, E.; Béni, S. Characterization of Diarylheptanoids: An Emerging Class of Bioactive Natural Products. *Journal of Pharmaceutical and Biomedical Analysis* **2018**, *147*, 13–34, doi:10.1016/j.jpba.2017.08.051.
35. Kuroyanagi, M.; Shimomae, M.; Nagashima, Y.; Muto, N.; Okuda, T.; Kawahara, N.; Nakane, T.; Sano, T. New Diarylheptanoids from *Alnus Japonica* and Their Antioxidative Activity. *Chemical and Pharmaceutical Bulletin* **2005**, *53*, 1519–1523, doi:10.1248/cpb.53.1519.
36. Li, J.; Liao, C.-R.; Wei, J.-Q.; Chen, L.-X.; Zhao, F.; Qiu, F. Diarylheptanoids from Curcuma Kwangsiensis and Their Inhibitory Activity on Nitric Oxide Production in Lipopolysaccharide-Activated Macrophages. *Bioorganic & Medicinal Chemistry Letters* **2011**, *21*, 5363–5369, doi:10.1016/j.bmcl.2011.07.012.
37. Riethmüller, E.; Tóth, G.; Alberti, Á.; Végh, K.; Burlini, I.; Könczöl, Á.; Balogh, G.T.; Kéry, Á. First Characterisation of Flavonoid- and Diarylheptanoid-Type Antioxidant Phenolics in Corylus Maxima by HPLC-DAD-ESI-MS. *Journal of Pharmaceutical and Biomedical Analysis* **2015**, *107*, 159–167, doi:10.1016/j.jpba.2014.12.016.
38. Lee, C.S.; Ko, H.H.; Seo, S.J.; Choi, Y.W.; Lee, M.W.; Myung, S.C.; Bang, H. Diarylheptanoid Hirsutenone Prevents Tumor Necrosis Factor-α-Stimulated Production of Inflammatory Mediators in Human Keratinocytes through NF-KB Inhibition. *International Immunopharmacology* **2009**, *9*, 1097–1104, doi:10.1016/j.intimp.2009.05.006.
39. Jiang, H.; Timmermann, B.N.; Gang, D.R. Use of Liquid Chromatography–Electrospray Ionization Tandem Mass Spectrometry to Identify Diarylheptanoids in Turmeric (Curcuma Longa L.) Rhizome. *Journal of Chromatography A* **2006**, *1111*, 21–31, doi:10.1016/j.chroma.2006.01.103.
40. Li, W.; Wang, S.; Feng, J.; Xiao, Y.; Xue, X.; Zhang, H.; Wang, Y.; Liang, X. Structure Elucidation and NMR Assignments for Curcuminoids from the Rhizomes of Curcuma Longa. *Magnetic Resonance in Chemistry* **2009**, *47*, 902–908, doi:10.1002/mrc.2478.
41. Woo, K.W.; Moon, E.; Kwon, O.W.; Lee, S.O.; Kim, S.Y.; Choi, S.Z.; Son, M.W.; Lee, K.R. Anti-Neuroinflammatory Diarylheptanoids from the Rhizomes of Dioscorea Nipponica. *Bioorganic & Medicinal Chemistry Letters* **2013**, *23*, 3806–3809, doi:10.1016/j.bmcl.2013.04.073.
42. Masuda, T.; Jitoe, A.; Isobe, J.; Nakatani, N.; Yonemori, S. Anti-Oxidative and Anti-Inflammatory Curcumin-Related Phenolics from Rhizomes of Curcuma Domestica. *Phytochemistry* **1993**, *32*, 1557–1560, doi:10.1016/0031-9422(93)85179-U.
43. Park, S.-Y.; Kim, D.S.H.L. Discovery of Natural Products from Curcuma Longa That Protect Cells from Beta-Amyloid Insult: A Drug Discovery Effort against Alzheimer's Disease. *J. Nat. Prod.* **2002**, *65*, 1227–1231, doi:10.1021/np010039x.
44. Nakayama, R.; Tamura, Y.; Yamanaka, H.; Kikuzaki, H.; Nakatani, N. Two Curcuminoid Pigments from Curcuma Domestica. *Phytochemistry* **1993**, *33*, 501–502, doi:10.1016/0031-9422(93)85548-6.
45. Park, B.-S.; Kim, J.-G.; Kim, M.-R.; Lee, S.-E.; Takeoka, G.R.; Oh, K.-B.; Kim, J.-H. Curcuma Longa L. Constituents Inhibit Sortase A and Staphylococcus Aureus Cell Adhesion to Fibronectin. *J. Agric. Food Chem.* **2005**, *53*, 9005–9009, doi:10.1021/jf051765z.
46. Dosoky, N.S.; Setzer, W.N. Chemical Composition and Biological Activities of Essential Oils of Curcuma Species. *Nutrients* **2018**, *10*, 1196, doi:10.3390/nu10091196.
47. Lin, X.; Ji, S.; Li, R.; Dong, Y.; Qiao, X.; Hu, H.; Yang, W.; Guo, D.; Tu, P.; Ye, M. Terpecurcumins A–I from the Rhizomes of Curcuma Longa: Absolute Configuration and Cytotoxic Activity. *J. Nat. Prod.* **2012**, *75*, 2121–2131, doi:10.1021/np300551g.
48. Núñez, N.; Vidal-Casanella, O.; Sentellas, S.; Saurina, J.; Núñez, O. Characterization, Classification and Authentication of Turmeric and Curry Samples by Targeted LC-HRMS Polyphenolic and Curcuminoid Profiling and Chemometrics. *Molecules* **2020**, *25*, 2942, doi:10.3390/molecules25122942.

49. Kuo, P.-C.; Cherng, C.-Y.; Jeng, J.-F.; Damu, A.G.; Teng, C.-M.; Lee, E.-J.; Wu, T.-S. Isolation of a Natural Antioxidant, Dehydrozingerone from Zingiber Officinale and Synthesis of Its Analogues for Recognition of Effective Antioxidant and Antityrosinase Agents. *Arch Pharm Res* **2005**, *28*, 518–528, doi:10.1007/BF02977752.
50. Imai, S.; Morikiyo, M.; Furihata, K.; Hayakawa, Y.; Seto, H. Turmeronol A and Turmeronol B, New Inhibitors of Soybean Lipoxygenase. *Agricultural and Biological Chemistry* **1990**, *54*, 2367–2371, doi:10.1080/00021369.1990.10870290.
51. Hong, C.H.; Kim, Y.; Lee, S.K. Sesquiterpenoids from the Rhizome OfCurcuma Zedoaria. *Arch Pharm Res* **2001**, *24*, 424–426, doi:10.1007/BF02975188.
52. Kuroyanagi, M.; Ueno, A.; Koyama, K.; Natori, S. Structures of Sesquiterpenes of Curcuma Aromatica SALISB. II.: Studies on Minor Sesquiterpenes. *Chemical & Pharmaceutical Bulletin* **1990**, *38*, 55–58, doi:10.1248/cpb.38.55.
53. Mohn, T.; Plitzko, I.; Hamburger, M. A Comprehensive Metabolite Profiling of Isatis Tinctoria Leaf Extracts. *Phytochemistry* **2009**, *70*, 924–934, doi:10.1016/j.phytochem.2009.04.019.
54. Su, B.-N.; Park, E.J.; Nikolic, D.; Vigo, J.S.; Graham, J.G.; Cabieses, F.; van Breemen, R.B.; Fong, H.H.S.; Farnsworth, N.R.; Pezzuto, J.M.; et al. Isolation and Characterization of Miscellaneous Secondary Metabolites of Deprea Subtriflora. *J. Nat. Prod.* **2003**, *66*, 1089–1093, doi:10.1021/np030081n.
55. Li, J.; Zhao, F.; Li, M.Z.; Chen, L.X.; Qiu, F. Diarylheptanoids from the Rhizomes of Curcuma Kwangsiensis. *J. Nat. Prod.* **2010**, *73*, 1667–1671, doi:10.1021/np100392m.